Ecological Indicators 186 (2026) 114850

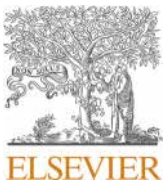

Contents lists available at ScienceDirect

Ecological Indicators

journal homepage: www.elsevier.com/locate/ecolind

How climate, fire types and topography drive forest biomass vulnerability to fires assessed from high resolution space-for-time analysis

Lilian Vallet [a,b,c,*], Florent Mouillot [a]

[a] CEFE, Univ Montpellier, CNRS, EPHE, IRD, 1919 Route de Mende, Montpellier, France
[b] French Environment and Energy Management Agency, 20 avenue du Grésillé BP 90406 49004 Angers CEDEX 01, France
[c] Forest and Rangeland Stewardship department, Colorado State University, Fort Colins, 80523, CO, USA

ARTICLE INFO

Keywords:
Vulnerability
Aboveground biomass
postfire dynamics
Space-for-time
remote sensing
fire ecology
GEDI
landsat
Forest
Random Forest
Driver

ABSTRACT

Climate change is driving the expansion of fire-prone areas and the intensification of wildfire events, threatening European forests. Yet, how this shift in fire regime might be more impactful on ecosystems lacks data-driven assessments of forest ecosystem vulnerability to this disturbance. We propose a comprehensive framework for assessing forest biomass vulnerability to wildfires across France, leveraging high-resolution tree height data and Landsat-based fire history reconstruction. We developed a new mapping of forest aboveground biomass (AGB) at 10m resolution, providing detailed insights into biomass distribution across various forest types. Additionally, we compiled a new database of fire polygons in France since 1984, encompassing 1762 fires, which serves as a critical resource for time since last fire and fire characteristics. Utilizing a space-for-time approach, we characterized post-fire drivers of biomass recovery, integrating species-specific fire response traits, fire characteristics, climatic conditions, and topographic variables. Our findings reveal significant regional variations, with temperate forests exhibiting higher vulnerability due to greater biomass exposure, lower resistance, and recovery rates, with local effects of topo-climates and fire size. The high-resolution mapping of quantitative vulnerability offers a robust tool for fire risk management, emphasizing the importance of considering post-fire recovery in carbon stock assessments. This work aims to inform decision-makers and enhance fire prevention strategies, contributing to sustainable forest management under changing climate conditions.

1. Introduction

Wildfire is one of the major disturbances affecting European forests (Senf & Seidl, 2020), and climate change may increase burned area in the existing fire-prone regions (Jones et al., 2022) but also expand to regions hardly affected by fires until now (Galizia et al., 2023; Senande-Rivera et al., 2022). Particularly, more frequent heat waves and prolonged drought might be responsible for these changes (El Garroussi et al., 2024; Ruffault et al., 2020), as recently observed during the 2022 fire season with a distinctive fire pattern toward the northern temperate forests of Europe (Rodrigues et al., 2023). Burned area then appears as the major indicator of interest to understand the underlying drivers leading to these extreme events (Abatzoglou et al., 2018; Jones et al., 2022). Additionally, wildfires and burned area are considered as an essential climate variable (ECV) (*GCOS | WMO*, 2024) and an essential biodiversity variable (EBV) (Pereira et al., 2013), highlighting the increasing scientific and societal awareness of the potential fire impacts on the environment, the climate and societies. Accordingly, assessments of fire impacts on wildlife habitat alteration and biodiversity (Brotons et al., 2005), tree cover and carbon stock loss (Patacca et al., 2023) have been conducted, aiming at providing ecosystem vulnerabilities to wildfires for decision makers as a supplementary index to burnt area alone (Oliveira et al., 2018).

Fire impacts on greenhouse gas emissions and terrestrial carbon stocks have rapidly emerged as an additional keystone impact to quantify (Kaiser et al., 2012; Van Wees et al., 2022), benefiting from the systematic burned area detection at global scale from remote sensing since 2001 (Chuvieco et al., 2019; Mouillot et al., 2024). Alongside these biogeochemical modeling of fire emissions, fire impact assessments started to account for post-fire carbon stock recovery (Yue et al., 2013), pointing out potential irrecoverabilities that could undermine climate mitigation goals within the next 40 years (Noon et al., 2021). Accounting for recovery time in the carbon balance of fire-prone ecosystems then appears as critical information. Considering this threat when

* Corresponding author at: CEFE, Univ Montpellier, CNRS, EPHE, IRD, 1919 Route de Mende, Montpellier, France.
E-mail address: lilian.vallet@cefe.cnrs.fr (L. Vallet).

https://doi.org/10.1016/j.ecolind.2026.114850
Received 4 April 2025; Received in revised form 16 March 2026; Accepted 5 April 2026
Available online 24 April 2026

evaluating and reporting extreme fire events, rather than its burned area alone, could then greatly improve the message to society and decision makers to prioritize safety interventions or management strategies (Oliveira et al., 2020). Assessing fire risk holistically offers a promising framework for generating tangible and quantitative information (Chuvieco et al., 2023) in this regard. The framework of risk assessment for a forest ecosystem following a natural disturbance integrates hazard, exposure and vulnerability components (Aven, 2011; Chuvieco et al., 2023; Coppola, 2015, Lecina-Diaz et al., 2021). In the context of fire impact on forest biomass, hazard represents the occurrence of fire; exposure refers to the quantity of forest biomass potentially affected by fire; and vulnerability expresses the degree to which a forest ecosystem is affected over time. Vulnerability reflects the forest's capacity to resist and recover when exposed to the fire. Thus, vulnerability can be considered as the absence of the exposed value over time.

Quantitatively applying this framework is, however, challenging (Angeler & Allen, 2016; Dakos & Kéfi, 2022; Ingrisch & Bahn, 2018; Rodrigues et al., 2024), both in quantifying the ecological values (Amador-Cruz et al., 2021) and how they can be assembled into a single index (Finney, 2005). Forest carbon storage, as an ecological value, is however more related to tangible information (expressed in tons of carbon), that should enable an objective application of the vulnerability framework. Efforts to compile data on fire-induced tree mortality (Cansler et al., 2020), understanding the underlying processes (Kavanagh et al., 2010), identifying key fire resistance plant traits (Moris et al., 2022; Pausas et al., 2018), and quantifying carbon stock alterations (Webb et al., 2024) during fire events, could provide a first step toward a quantitative integration of resistance. Carbon stock recovery time then depends on plant regeneration strategies from fires (Archibald et al., 2019), from individuals through vegetative reproduction (resprouting) to seed germination from fire-resistant seed bank or through dispersal from unburned neighboring forest patches. It also depends on the growth rate of species, as implemented in forest models (Morin et al., 2021; Schwörer et al., 2014) modulated by climate constraints (Shen et al., 2025). Yet, these pieces of conceptual framework, local information, or empirical and process-based models lack large scale data-driven assessment methodologies to provide stakeholders with quantitative and objective mapping of forest carbon stock vulnerability to wildfires.

Advances in remote sensing managed to step further forest vulnerability assessment to regional or global level, mostly through time series of spectral indices following fires, or space-for-time analysis across landscape with contrasting time since last fire. The use of spectral indices (Ermitao et al., 2024; Ouattara et al., 2025; Shen et al., 2025) mostly driven by foliage characteristics, partially relate to forest carbon stock dynamic with a faster recovery of foliage than wood biomass (Prodon & Diaz-Delgado, 2021), and does not necessarily follow forest recovery (Celebrezze et al., 2024). Recent global access to fine resolution Lidar data now provides tree height (Potapov et al., 2021) and tree cover information (Hansen et al., 2013), which are more correlated than spectral indices to forest tree biomass. Lidar data are, however, available only since 2019 on a global scale. This information could effectively quantify exposed biomass (Vallet et al., 2023) and biomass loss and mortality rates (Fernández-Guisuraga et al., 2022) for the 2020–2022 fire seasons in Europe, for example, but prevent diachronic investigations of vegetation recovery over a long period. Using these data, Forzieri et al. (2021) proposed a European scale forest vulnerability assessment, but based on biomass loss alone, omitting the recovery component. Space-for-time analysis can effectively relate tree height with time since last fire across various biomes, covering single fire events (Epstein et al., 2024) to large territories (White et al., 2022) where long-term fire data were available, but did not convert tree height into carbon stocks. Yet, no convincing studies proposed a quantitative vulnerability assessment and mapping of forest carbon stocks at the territory scale seen through the lens of forest resistance and recovery. This kind of evaluation could be a useful tool for decision makers and an objective quantification of fire impacts when they happen.

Following the distinctive 2022 fire season in France with 42,520 ha burned and abnormally affecting the non-mediterranean part of the country less prone to fires (Vallet et al., 2023), France launched in July 2023 its new national strategic reinforcement law for fire prevention (LEGIFRANCE, 2023) aiming at a better characterization of fire hazard and forest vulnerability (Rivière et al., 2023). This strategy aligns with the wider European (Berchtold et al., 2025) and global (Oliveras Menor et al., 2025) strategies for an integrated fire management aiming at reconsidering fires beyond the simple fire hazard. Considering these objectives, we propose to develop and provide a comprehensive and robust quantitative framework of forest carbon stock vulnerability to fire accounting for their key drivers. This objective timely coincides with the recent delivery of fine resolution tree height mapping over France (Schwartz et al., 2025) to produce a forest biomass map, and accessibility to open access fire history reconstruction tools from remote sensing (Roteta et al., 2021) filling the gap of historical fire data still lacking in the country. We thus aim at concomitantly generating a Landsat-based fire perimeter dataset since 1984 to perform a space-for-time biomass analysis and provide a methodological framework to deliver a quantitative and objective fire vulnerability mapping of forest carbon stock at the national level.

2. Materials and methods

2.1. Study area

Our study covers the France metropolitan area (41.38N-51.09N, 4.76W-9.55E)for which a national forest biomass map was recently delivered (Schwartz et al., 2023), covering a wide range of forest biomes from Mediterranean to temperate, and highly affected by unusual 2022 fire season leading to the July 2023 new law for reinforcement on fire prevention and firefighting (https: //www.legifrance.gouv.fr/loda/id/JORFTEXT000047805414). The French metropolitan territory features a high diversity of forest types and fire regimes (Fig. 1). Fires occur mainly in the southeast of France, where the climate is Mediterranean. On average, 4,812 ha of wildland has been burnt in this area every year since 2006 (*BDIFF*, 2026; Vallet et al., 2023). There is considerable interannual variability in the area burnt (SD = 3,855 ha), depending on climatic conditions, with some record years such as 2017 (15,660 ha). This area includes low forests of evergreen oak (*Quercus ilex, Quercus suber*) or Pine (*Pinus halepensis, Pinus nigra*) as well as areas of sclerophyllous vegetation (shrubland, maquis, guarrigue).

The southwest of France is also affected by fires. Even though this area is relatively less affected than the Mediterranean basin (burnt area 2006-2019 = 494 ha.yr-1), some fire events can reach large areas (Landiras fire in 2022 = 12,140 ha), resulting in significant total burnt areas (in 2022, 26,858 ha burnt) (BDIFF, 2023; Vallet et al., 2023). This region is characterized by a maritime pine (*Pinus pinaster*) forest intensively managed for timber production.

The northern part of France is less fire-prone, but during prolonged drought and heatwave events, fires can occur and cause large burnt areas, as in 2019 (3,035 ha) or 2022 (7,813 ha) (BDIFF, 2023; Vallet et al., 2023). This area is dominated by temperate forests with contrasting management practices. The main tree species are oak (*Quercus petreae, Quercus robur*), beech (*Fagus sylvatica*), Scots pine (*Pinus sylvestris*), spruce (*Picea abies*) and fir (*Abies alba*).

2.2. Vulnerability assessment

We quantified the fire vulnerability and its components for each forest pixel (Fig. 2). Based on the conceptual scheme proposed by Chuvieco et al. (2023) for European forest vulnerability assessment to fire, the Exposure (*E*) corresponds to the initial state of the vegetation before disturbance, i.e. the AGB map produced for the year 2020 in our scenario. The Resistance (*R*) corresponds to the amount of biomass that

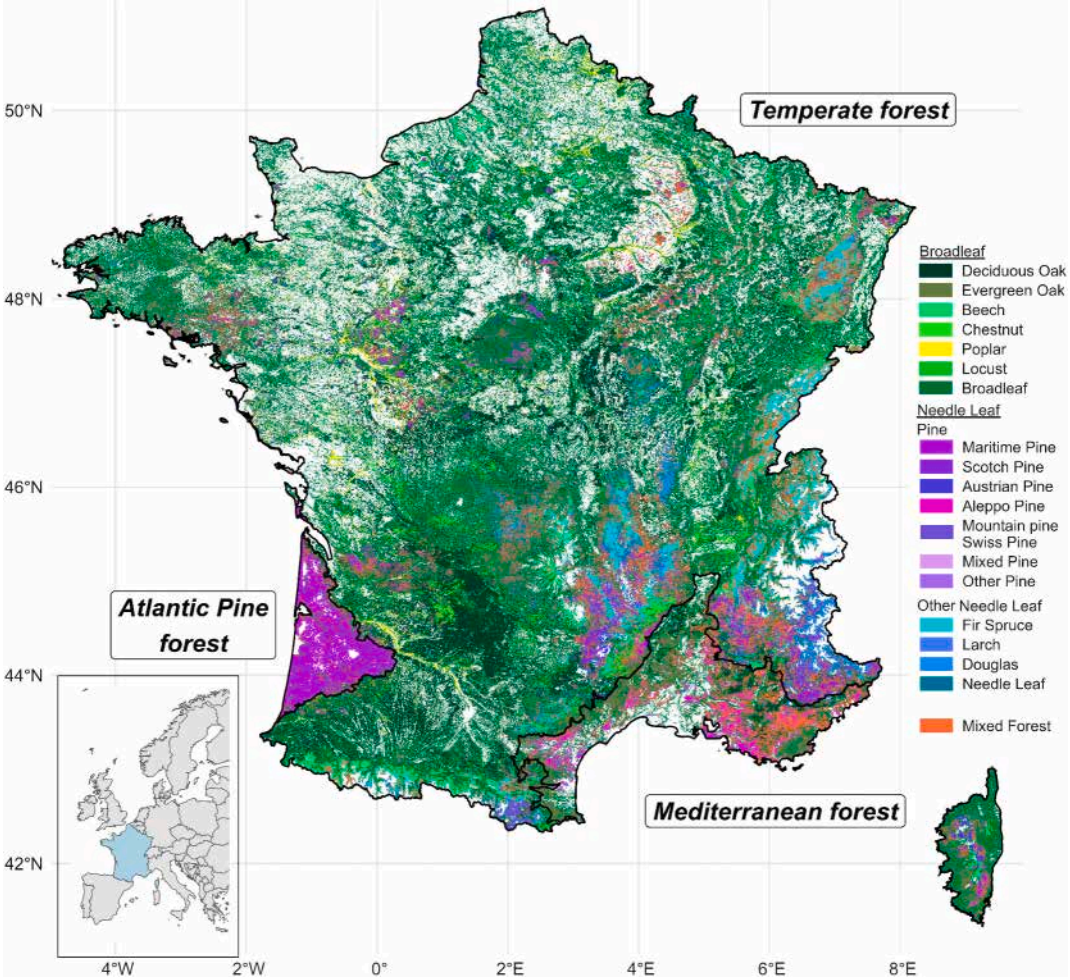

Figure 1. Map of the 19 forest classes in France (IGN, 2018). The classification is separated into Broadleaf and Needle leaf and based on the National Forest Inventory. The resolution of the initial data is 10m. For better visualization, the data were resampled to 500m resolution and represent the dominant forest class. The French map and the snapshot showing France within the European continent follow the WGS84 projection.

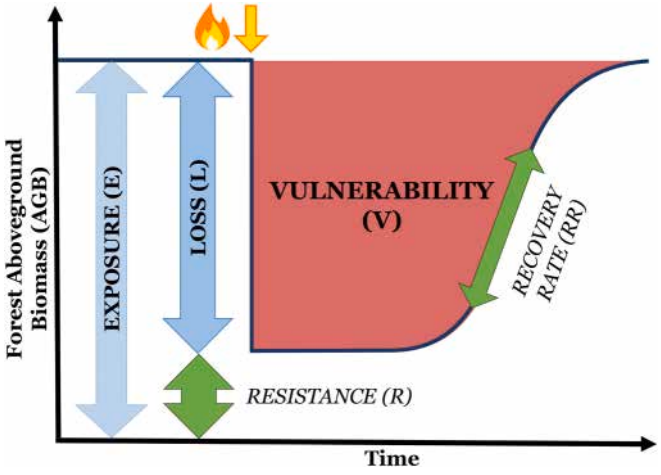

Figure 2. Conceptual scheme of vulnerability to disturbance. Here, we take the example of forest biomass vulnerability to fire, but this theoretical scheme could be applied to other ecological values and other disturbance types.

survived the fire ($R = AGB_{t=1}$). The recovery rate (RR) corresponds to the annual biomass gain after fire, i.e., the difference in AGB between two consecutive years t and t-1. It is calculated for each year (t) over the simulated period (T=35 years).

$$RR_t = AGB_t - AGB_{t-1}$$

Vulnerability (V) expresses the absence of exposed biomass over time. It depends on the resistance and recovery rate of the forest. It corresponds to the integral over the post-fire biomass recovery curve. It can thus be expressed as the sum of the exposure minus annual biomass (AGB_t) predicted over the period T.

$$V = \sum_{t=1}^{T} E - AGB_t = E^*T - \left(R + \sum_{t=2}^{T} AGB_{t-1} + RR_t\right)$$

2.3. Fire data

To process our space-for-time analysis over the period 1984-2022, and in absence of any consistent and homogeneous database over the country, we delineated fire polygons using the semi-automatic Burned Area Mapping Tools (BAMTs) within the Google Earth Engine platform (Bastarrika et al., 2014; Roteta et al., 2021). We focused our mapping effort on fires larger than 10 ha (Fig. 3). BAMTs relies on the use of atmospherically corrected and orthorectified satellite images (Landsat since 1984 and ESA Sentinel-2 since 2016) to derive three spectral indices: Normalized Differential Vegetation Index (NDVI) (Rouse et al., 1974), Normalized Burn Ratio (NBR) (Key & Benson, 1999), and NBR2 (García & Caselles, 1991). To localize fire events spatially and

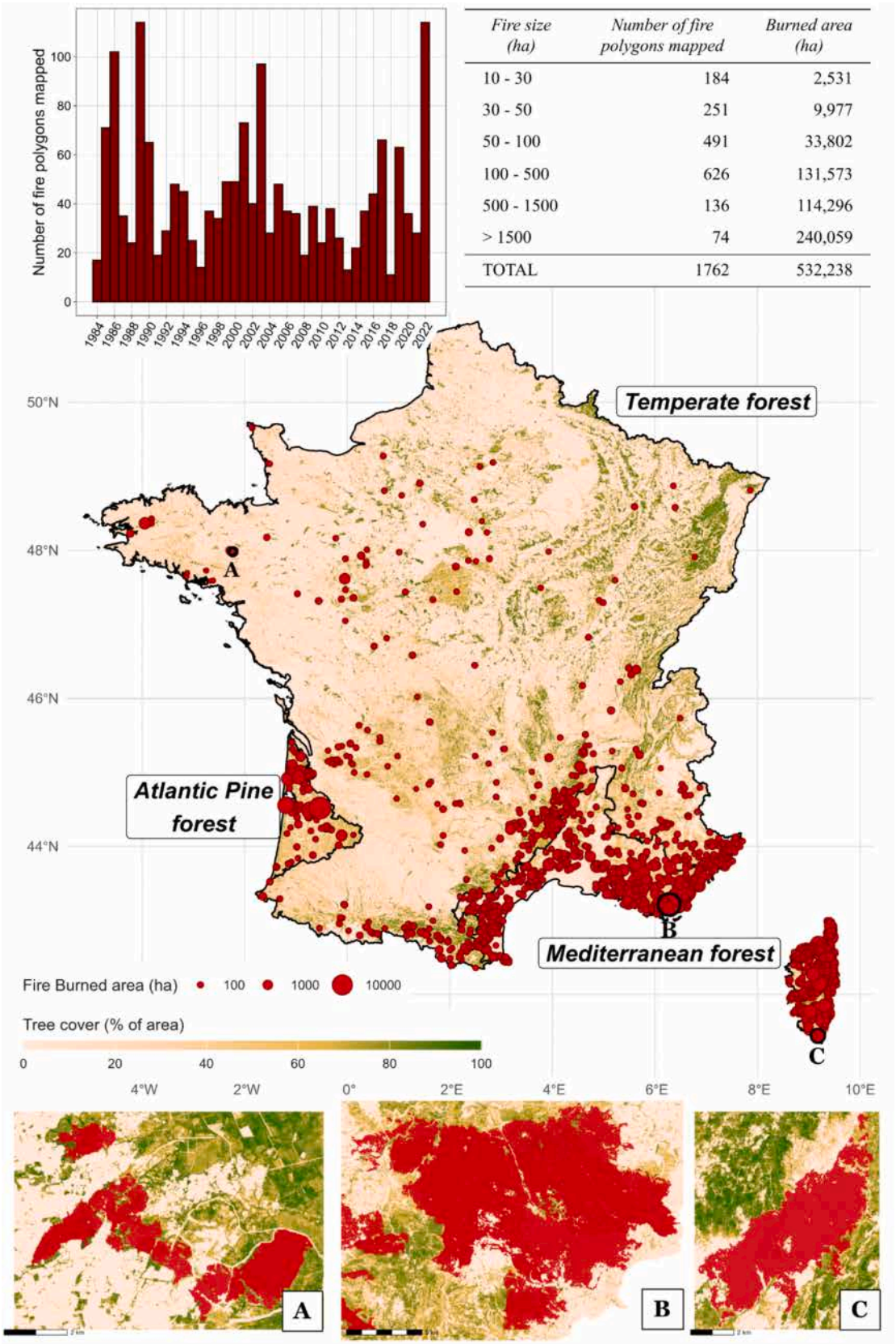

Fire size (ha)	*Number of fire polygons mapped*	*Burned area (ha)*
10 - 30	184	2,531
30 - 50	251	9,977
50 - 100	491	33,802
100 - 500	626	131,573
500 - 1500	136	114,296
> 1500	74	240,059
TOTAL	1762	532,238

Figure 3. Fire polygon data for France between 1984 and 2022. Top-left: Number of polygons mapped per year. Top-right: Number of polygons mapped and total burnt area by fire size class. Middle: Fire polygon distribution map. Bottom: local snapshot (A,B and C) showing the fine resolution of fire polygons overlapped with tree cover (Sexton et al., 2013).

temporally, we took advantage of the national fire occurrence database (*BDIFF*, 2026). Fires are referenced with their date and municipality of occurrence since 1973 for the Mediterranean area and since 2006 for the whole country. We also leveraged 71 fire occurrence information from grey literature to map polygons absent from the national inventory and mostly in the non-Mediterranean area over the 1984-2005 period. We used this information to identify the pre- and post-fire periods for capturing changes in the three spectral indices, represented by an RGB color scale. More precisely, the pre-fire period runs from the beginning of the year (January 1st) to the referenced fire date, and the post-fire period extends from the fire date to several weeks, to ensure enough cloud-free satellite images. A visual inspection then allows to manually delineate a training zone of burnt and unburnt pixels for a random forest classifier (Belgiu & Drăguţ, 2016). This step, which is not included in current automatic methods, ensures fire-specific adjustments and visual inspection to follow the international standards advocated by the CEOS Working Group on Calibration and Validation of remote sensing datasets (Franquesa et al., 2020).

We could map 1,762 fires between 1984 and 2022, for a total burnt area of 532,238 ha. Most of the fires affected an area less than 100 ha (n = 926), but accounted for only 46,310 ha, while the 74 fires > 1,500 ha account for 240,059 ha.

2.4. Aboveground biomass data

To quantify forest carbon stocks exposed to fires, we first aimed at obtaining the forest aboveground biomass (AGB) over France at a fine resolution. We relied on the spatial classification of forest into 19 forest classes (FC) (*IGN: BD FORET*, 2018) (Fig. 1) categorized by the national forest inventory, taxonomically more or less precise. FC can indeed correspond to one species (maritime pine, chestnut, poplar, …), two species (fir & spruce, Laricio pine & black pine), a genus or part of a genus (pine, deciduous oak, evergreen oak), a phylum (conifer, deciduous) or a broader classification (mixed forest).

We then leveraged forest plot data from the national forest inventory (IGN, 2018) since 2005 on more than 100,000 plots, which we grouped to a corresponding FC. A plot is assigned to a forest class (FC) when at least 75% of its trees match the class description. Thus, a plot can belong to several FC. For example, a plot dominated by maritime pine species corresponds to both 'Maritime Pine' and 'Coniferous' FCs. Plot data were then used to construct a first allometric relation (Fig. 4). This allometry predicts the Diameter at Breast Height (*DBH*) of a single tree as a function of its height (*H*) for each forest class *c* and is affected by the parameter α_c.

$$DBH = \frac{\alpha_c H^2}{\pi} \quad (1)$$

The second allometric relation used in this study was derived from the R 'allodb' package (Gonzalez-Akre et al., 2022). This package compiles information from scientific literature on many taxa and biomes. This relation estimates the biomass of a tree (AGBt) as a function of its DBH (Eq. 2). For each FC, we selected the dominant species of the corresponding plots to obtain this relationship.

$$AGBt \sim f_c(DBH) \quad (2)$$

The last allometric relationship was derived from plot data and established the relationship between tree biomass ($AGBt_c$) and surrounding tree density (D_c). We selected only plots corresponding to a closed forest. Then, for each FC, we applied equation (2) to all individuals in the corresponding plots and calculated the plot's tree density (Eq. 3). This allowed us to extract the parameter k_c influencing this relationship, in accordance with the self-thinning rule (Puntieri, 1993).

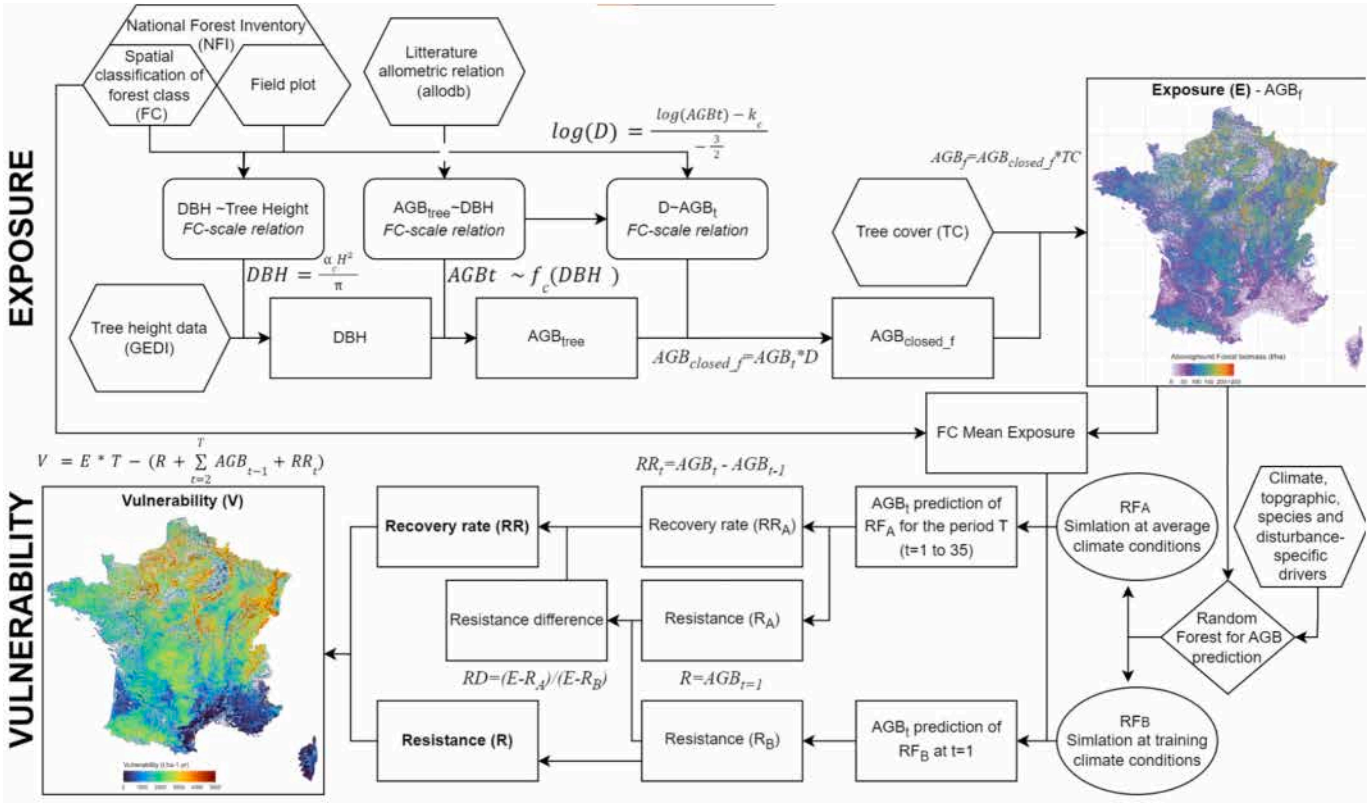

Figure 4. Processing chain of Exposure and Vulnerability assessment. Hexagonal boxes correspond to external input data. Round-edged rectangular boxes are relations obtained between input data. Rectangular boxes correspond to values obtained from input data and relationships. DBH: Diameter at Breast Height, AGB: Aboveground biomass, D: Tree density, RF: Random forest.

$$log(D) = \frac{log(AGBt) - k_c}{-\frac{3}{2}} \quad (3)$$

These three relationships are then combined and applied to the fine resolution vegetation height map (Schwartz et al., 2025) over France following Eq. 4. This data has a resolution of 10 m and is derived from a combination of optical (Sentinel-2), SAR (Sentinel-1) and aerial lidar (GEDI) data (Dubayah et al., 2022). For each pixel (H_x) of forest class c with a height greater than 3m, we obtain the forest AGB ($AGBf$) by multiplying the AGB of a tree ($AGBt$) by the tree density (D) (Eq. 4).

$$AGBf = f_c \left(\frac{\alpha_c H^2}{\pi}\right)^{\frac{1}{3}} \times 10^{\frac{2k_c}{3}} \quad (4)$$

We then estimated the aboveground biomass of forests throughout the country. At this point, this biomass corresponds to closed forests only. Consequently, we multiplied the biomass estimate by the value of the forest cover to consider the openness of the forests (*Copernicus Land Monitoring Service*, 2026). This information on aboveground forest biomass (AGBf) will be further referred to as exposure (E) in the rest of the study.

The aboveground biomass (AGB) layer obtained was not directly validated here, as it is derived from the GEDI-based FORMS tree height dataset (Schwartz et al., 2023). This product has been validated across France using both airborne LiDAR acquisitions and extensive field inventories, demonstrating high accuracy in forest canopy height retrieval. The subsequent conversion from canopy height to AGB relies on empirical allometric relationships calibrated with National Forest Inventory (IFN) plots collected across France since 2005. These field data provide ground-based reference for biomass estimation and ensure consistency with national carbon stock assessments. Together, these validated inputs ensure the reliability of the AGB data used as the response variable in the following analysis.

To provide an objective assessment of value ranges and spatial patterns, we compared our 10 m AGB map with three recent, independently-produced AGB products that differ in spatial extent and native resolution. Schwartz et al. (2023) is a national (France-wide) product at 30 m, while Miettinen et al. (2025) and Santoro et al. (2026) are pan-European products provided at 10 m and 20 m, respectively. When necessary, products were reprojected and resampled to the 10 m grid using nearest-neighbour resampling to preserve original values and avoid smoothing artefacts. We then extracted a systematic sample of 100,000 co-located pixels within the common valid domain and computed agreement metrics (RMSE, MAE and R^2) between our map and each comparison product.

2.5. Post-fire dynamic drivers of biomass recovery

To quantify the vulnerability of forest AGBf to fire at fine resolution and including local variations, we identified and collected variables that could function as drivers of post-fire biomass dynamics (Table 1). We selected keystone variables as fire characteristics, climate, topography, species, or other disturbance events. Except for fire-specific data, these variables were collected and aggregated for the whole study area. We then extracted those data for each AGB pixel with a resolution of ~10m. Where data was available at a different resolution, resampling was conducted using the nearest neighbor method, except for the Digital Elevation Model data, for which a bilinear interpolation method was used.

2.5.1. Fire characteristics

The burn date provided by the national fire inventory BDIFF was used to obtain two variables: the month in which the fire occurred (*Month*) and the time since the last fire (*Time since fire*). The latter corresponds to the duration, expressed in years, between the year of the fire and 2020, the year to which the AGB exposure data corresponds to, and was used as the recovery time. *Month* was used to evaluate how fire seasonality could affect loss and regeneration (Tangney et al., 2022). From fire polygons, *Edge distance* (in m) is computed with the R package terra (Hijmans, 2025) as the distance between a burnt pixel and the closest unburnt one to test how proximity to undisturbed forest could fasten the recovery (Trang et al., 2023). We also computed *time between disturbances* (in years) as minimum period between two successive fires during the 1984-2020 period, as a critical period below which juvenile

Table 1
Environmental and disturbance predictors used to model post-fire aboveground biomass vulnerability. 15 explanatory variables are included in the analysis, grouped into fire characteristics, climate drivers, topographic variables, and species traits. Variables were resampled to the analysis grid before modelling and species-trait values and their primary references are detailed in Table A1.

Category	Variable	Definition	Units	Native resolution	Period	Source (dataset)
Fire characteristics	**Time since fire**	Years between fire year and 2020 (AGB reference year)	years	event attribute	fire year	**BDIFF** + mapped fire polygons
	Month	Month of fire occurrence	month (1–12)	event attribute	fire year	**BDIFF**
	Edge distance	Distance from a burned pixel to nearest unburned pixel / fire edge	m	derived from polygon geometry	fire year	mapped fire polygons
	Severity (dNBR)	Burn severity index (difference NBR pre vs post fire)	unitless index	30 m	fire year	Landsat-based dNBR method
	Time between disturbances	Time between the focal fire and the previous disturbance (fire or other disturbance)	years	event attribute	since 1984	Fire polygons + European disturbance map
Climate drivers	**Temperature mean**	Mean annual air temperature	°C	0.1° (~9 km)	1984–2019	ERA5-Land
	Precipitation mean	Mean annual precipitation	mm/yr	0.1° (~9 km)	1984–2019	ERA5-Land
	SPEI min	Minimum drought intensity in first 5 post-fire years (6-month SPEI)	SPEI units	computed from 0.1° climate	1984–2019	ERA5-Land + SPEI method
Topographic variables	**Aspect**	Slope aspect (north–south exposure)	degrees (°)	1 m DEM	static	RGE ALTI® DEM
	CTI	Compound topographic index (proxy for moisture accumulation)	unitless	1 m DEM	static	RGE ALTI® DEM + CTI formulation
	AWC	Available water capacity (0–2 m soil depth)	mm	~90 m	static	Soil AWC dataset
Species traits	**Bark thickness**	Trait proxy for fire resistance	cm	forest-class attribute	static	Literature compilation (See Table A1)
	Resprouting ability	Probability/ability of resprouting after fire	proportion or %	forest-class attribute	static	Literature compilation (See Table A1)
	Serotiny capacity	Fraction of individuals/seed bank serotinous	proportion or %	forest-class attribute	static	Literature compilation (See Table A1)
	Dispersal distance	Typical seed dispersal distance	m	forest-class attribute	static	Literature compilation (See Table A1)

individuals might not have time to produce seeds and regenerate after the fire (Ermitao et al., 2024; Koutsias et al., 2024; Mouillot et al., 2001).

In addition, the differential Normalized Burn Ratio (dNBR), has been assembled as an index of *Severity* affecting vegetation dynamic (Cardil et al., 2019; Koutsias et al., 2024). This index is obtained by comparing pre- and post-fire spectral bands from Landsat 5, 7 and 8 missions. We used the dNBR extraction method provided by (Parks et al., 2018) in Google Earth Engine, to map the severity index over all the 1588 fires before 2020 at a 30m resolution.

2.5.2. Climate

To consider the climatic impact on post-fire dynamics, we relied on the ERA5-Land hourly reanalysis dataset (Hersbach et al., 2020). We collected temperature at 2m and total precipitation data for the period 1984-2019. We computed the mean annual temperature (*Temperature mean MAT*). We also extracted the mean annual precipitation (*Precipitation mean MAP*). This information was obtained on each pixel of 0.1° (~9 km) as an index of local productivity acknowledged to drive tree rate of growth (Reich et al., 2014), species maintenance (Elvira et al., 2026) and regeneration capacities (Baudena et al., 2020).

To investigate the effect of drought occurring in the first few years after the fire, we computed a drought index on the same hourly climate data. The selected drought index is the Standardized Precipitation-Evapotranspiration Index computed with the R package SPEI (Beguería et al., 2014; Vicente-Serrano et al., 2010), as a standard flexible index previously used for post fire regeneration analysis (Andrus et al., 2022, Viana-Soto et al., 2020). For each fire, we first calculated monthly temperature and precipitation from the ERA5-LAND dataset. Then we calculated the potential evapotranspiration value using the function of Thornthwaite (1948) and the 6month-SPEI index over the entire 1984-2019 period. Finally, we extracted the 6month-SPEI values over the 5 years following the burn date (4 years for the 2019 fires) and retained the lowest 6month-SPEI value (*SPEI min*) occurring during that time frame following (Blanco-Rodríguez et al., 2023).

2.5.3. Topographic variables

We extracted topographic variables from a digital elevation model at a resolution of 1m (RGE ALTI® | Géoservices, 2026). We extracted the aspect (*Aspect*), expressed in degree (°) between 0 (North) and 180 (South) as a major local modifier of solar radiation and subsequent information as evapotranspiration and drought, or soil heat load (Liu et al., 2022). Based on the DEM, we calculated the compound topographic index (*CTI*) (Sørensen et al., 2006). This unitless index is used to identify precipitation accumulation zones and as a proxy for soil moisture in hillslopes, with a high CTI value corresponds to a valley floor, while a low CTI value corresponds to a ridgeline, previously identified as a significant driver of post-fire recovery (Holik et al., 2025). We also leveraged Available Water Capacity (AWC) data (Roman Dobarco et al., 2022). This variable corresponds to the amount of water a soil can contain and be used by plants, and considered as a key variable driving tree growth (Bončina et al., 2023; Schneider et al., 2021). This database is provided at a resolution of ~90m and for a depth of 2m. As this data is not available for Corsica, we set a value of 50 mm for this region, close to the median value for southeastern France.

2.5.4. Species traits

To investigate the species-specific influence on post-fire dynamics, we considered species by four fire-related functional traits and allowed the species to be classified by their functional distance rather than a category, and assuming functionally similar species have similar dynamic (Rocha et al., 2011). Trait values are taken from scientific literature and are presented in Table A1.

The first trait is the *Bark thickness*, expressed in centimeters. This trait is considered as a proxy for the species' resistance to fire (Pausas, 2015), since sufficient bark thickness enables the individual to protect its hydric system from high temperatures.

The second trait is *Resprouting ability*, expressed as a percentage. FC capable of resprouting hold dormant meristems, generally root meristems, which can be activated after a fire to allow regrowth (Pausas et al., 2018).

The third trait is the *Serotiny capacity*, expressed as a percentage. Serotinous FCs, mostly pines, hold their seeds in cones whose opening is triggered by high temperatures occurring during fires and allowing post fire germination (Lamont et al., 2020).

The fourth trait is *Dispersal Distance*, expressed in meters. This trait corresponds to the average distance at which a species can disperse its seeds and can colonize a burned area from external individuals (Costa et al., 2025). It depends on seed size and dispersal mode (anemochory, zoochory, aquachory, etc.) (Lososova et al., 2023).

2.5.5. Data filtering

To perform our forest recovery analysis after fire disturbance, we had to ensure that the burnt pixels corresponded to the latest disturbance, by confronting our fire data with the European forest disturbance map (Senf & Seidl, 2020b) assembling all disturbances affecting European forests (insect attacks, clear-cutting, etc.). We have thus retained only the burnt pixels of our polygons with a date more recent or equal to that present in this European disturbance map. For each burnt pixel, we extracted the period between the date of the fire and the date of the last disturbance, either from the European disturbance map or from a previous burnt pixel (*Time between disturbance*). When disturbance recurrence was absent, i.e., no fire or other disturbance had preceded the fire since 1984, we set the '*time between disturbance*' variable at 100 years.

Out of the 462.472 ha burnt from our fire history reconstruction from 1984 to 2019, we have retained only those pixels belonging to one of the 19 FCs and not subsequently disturbed. In the end, 126,336 ha were retained for the study of post-fire forest dynamics.

2.6. Temporal biomass dynamics modelling

A Random Forest regression model was built to predict forest AGB from explanatory variables. This model was built upon the 15 topographical, climatic, species trait and fire characteristics variables mentioned above. The central variable in this analysis is the time since last fire, enabling us to simulate the post-fire temporal dynamics of biomass. The model was built using the R package 'ranger' (Wright and Ziegler, 2017) and is based on the individual burnt pixels, i.e., 11,485, 138 observations. To balance predictive accuracy with computational efficiency, we manually tested several combinations of Random Forest parameters (mtry, min.node.size, and num.trees) on representative subsets of the dataset. The final configuration (num.trees = 500, mtry = 3, min.node.size = 5) provided the best compromise between accuracy, measured by the root mean square error (RMSE), and processing time. This balance was crucial given that the model was trained and applied at a 10 m spatial resolution across the entire French territory for multiple time steps. This dataset was divided into a 90/10 ratio so that the first part was used to train the model and the second to test its accuracy, which still ensured more than one million independent observations for model evaluation. Model performance was evaluated on the 10 % independent test dataset using the coefficient of determination (R^2) and the root mean square error (RMSE), computed as:

$$\mathrm{RMSE} = \sqrt{\frac{1}{n}\sum_{i=1}^{n}(y_i - \hat{y}_i)^2}$$

where y_i and $\hat{y}_i$ denote observed and predicted AGB values, respectively, and n is the number of observations.

The model was applied to the test dataset and compared with biomass observations to estimate its performance. We extracted the R^2 reflecting the difference between estimated and observed biomass values. In turn, we extracted the partial (marginal) dependence curves from the Random Forest model for each of the 15 explanatory variables,

describing the isolated average effect of each variable on predicted AGB while holding all others constant. To make a visual comparison of each variable, we scaled these values so that the minimum value predicted by the variable is equal to 0.

This biomass estimation model as a function of time since last fire was then used to map forest vulnerability across France. To achieve this, we applied our model to explanatory variables for different time steps since the last fire. More specifically, we applied our model with a time since last fire equals to 1, 5, 10, 15, 20, 25, 30 and 35 years. For each time step, topography, species and mean climate were kept constant. For disturbance-related variables, we fixed the averaged values to provide a homogeneous vulnerability map to a mean similar fire event, rather than to local fire regimes. We set the month of July, as it corresponds to the largest burnt surface in the training set, the distance to the edge at 300m to avoid an edge effect and to consider a fire of at least 20ha, the severity (dNBR) at 300 to consider a fire of moderate severity and a time between disturbances equal to 100 years to remove the effect of disturbance recurrence. The last variable to be set was the effect of drought following fire (SPEI min), which we set to 0 to account for mean drought conditions.

For the first time step (t=1) we simulated ABG with two different climate inputs to assess forest resistance: one with the actual average climate gradient (RF_A in Fig. 4) and one where we set all pixel climate at the same median climate conditions of the training dataset (RF_B in Fig. 4). Using this median climate over the national territory makes sure that resistance is assessed for fire prone climate conditions, rarely occurring in the northern part of the country. Resistance for these two climate scenario R_A and R_B correspond to the ABG at time t=1. Recovery Rate (RR_A) was estimated by the yearly increase of ABG over time with average climate conditions (RF_A). The actual recovery rate (RR) was finally obtained by rescaling RR_A to the ratio between biomass losses between scenario A and B, as AGB_0-R_A and AGB_0-R_B. This corresponds to running a scenario in which the whole of France burns under the conditions observed under fire-prone conditions and recovering over 35 years under average conditions.

Since our model simulates the dynamic of an average forest based on explanatory variables and might omit some local environmental heterogeneity, we finally corrected the model's output values according to initial exposure (remotely sensed biomass). More precisely, we extracted the ratio between the exposure of each pixel and the average biomass of its FC. We then multiplied the model's predicted biomass by this ratio to consider the local deviation between the simulated biomass of a given pixel and the average biomass of the FC.

3. Results

3.1. AGB map

Our first result was to develop a map of the forest AGB throughout France for the year 2019, based on tree height data and field data (Fig. 5), to be used as a biomass exposure map to fire. At the national level, AGB varies significantly across FC and along the climate gradient. AGB is the highest in the north of the country, in temperate forests, with an average value of 110.9 tDM/ha (DM: dry matter) and reaching values above 250tDM/ha. In the south, in Mediterranean forests, biomass is much lower, with an average value of 32.0 tDM/ha and mostly varying between 30 and 80 t/ha. In the southwest, in the intensively managed Landes forest, biomass density is also low, with an average of 53.4 tDM/ha.

Our biomass estimation method enabled us to capture differences in biomass density among species—an outcome not achievable with tree height data alone. Temperate broadleaf species (beech, deciduous oak, fir, spruce) experience high biomass densities with, for example, the average values of beech (deciduous oak or fir and spruce, reaching respectively 134.8 tDM/ha, 108.8 tDM/ha, and 125 tDM/ha. Mediterranean species have much lower biomass densities, with on average 52.7 tDM/ha for evergreen oak or 30.7 tDM/ha for aleppo pine, due to the openness of the forest. Overall, pines experience low biomass densities from an average value of 27 tDM/ha for the “other pine” class to 71.6 tDM/ha for the “Mountain pine, Swiss pine” class. The dispersion of AGB values is lower for FCs composed of a single species than for those composed of a large group such as "Broadleaf" or "Needle leaf".

We also observed that the relation between AGB and tree height differs between forest classes (Fig. 6). While Schwartz et al (2023) consider a single relationship, being only different between needle leaf and broadleaf, we obtained more species-specific information. For example, although evergreen oaks reach heights of only 10m, their biomass density is higher than other broadleaf for a given height. Poplars, on the other hand, show a lower biomass density. For example, evergreen oaks show a density of 100 t/ha for a height of 11m, whereas this density is reached for trees of around 25m for poplars. Schwartz et al (2023) proposed a single density of 100t/ha for a height of 15m, regardless of the broadleaf species considered. We also note that needle leaf classes generally have lower biomasses than broadleaf relative to their height. Our biomass estimate for these FCs is lower overall than that of Schwartz et al. (2023), except for the Mountain Pine, Swiss Pine class.

To further assess the plausibility of the spatial patterns and magnitude of our AGB estimates, we compared our 10 m AGB map with three independent AGB products available over France (Fig. 7). At the pixel scale (100,000 co-located samples over the common valid domain), our map shows the strongest agreement with Schwartz et al (2023) (R^2 = 0.82; RMSE = 42.23 t/ha; MAE = 30.50 t/ha), consistent with the fact that both approaches rely on the same canopy height information over France. Agreement with the two pan-European products is lower (Miettinen et al., 2025: R^2 = 0.25; RMSE = 73.94 t/ha; Santoro et al., 2026: R^2 = 0.22; RMSE = 67.67 t/ha), and these products generally display smoother spatial patterns and lower local maxima in high-biomass stands. In contrast, our product retains finer spatial texture at 10 m and reaches higher AGB values in dense temperate forests, which likely reflects the use of forest-class-specific allometries calibrated for French forest conditions rather than generalized relationships fitted at continental scale.

3.2. Post-fire dynamic of biomass

Based on the forest biomass exposure map previously produced, we could process a space-for-time analysis and model post fire recovery as a function of time since last fire and other contributive variables (Fig. 8 and A2). Among the different types of biomass recovery drivers, fire-related characteristics have a significant effect on post-fire biomass (Fig. 8, red graphs). Time since last fire, the central variable in our analysis, appears to positively correlate with predicted AGB, confirming the actual biomass recovery across time. The average effect of the variable predicts a difference in biomass (dAGB) of 14.5 t/ha between year 1 and 35 after the fire. We additionally identified here that the month of fire occurrence has a non-linear relationship with the predicted AGB. Summer fires (June, July, and August) tend to promote lower biomass than fires burning during the rest of the year (dAGB=4.18 t/ha). May, September, and October fires also promote lower biomass than winter and spring fires (dAGB=3.7 t/ha), although higher than summer fires (dAGB=1.7 t/ha). we could also show that the distance to the edge shows a strong negative effect on the predicted AGB: the distance of the burnt pixel from the edge of the fire results in a reduced predicted AGB (between 0 and 300m, dAGB=9.8 t/ha). Severity and fire return intervals seem to show a slightly negative effect on AGB: dAGB=2.4 t/ha between DNBR 0 and 200 and dAGB = 2.8 t/ha between a succession of two disturbances at 1 and 100 years.

Climatic conditions in the burnt pixel act as strong drivers of post-fire biomass dynamics. Firstly, rainfall has a strong positive effect on the predicted AGB: an increase of 30.4t/ha is observed between an average annual precipitation of 600 mm and one of 1300 mm. Mean annual

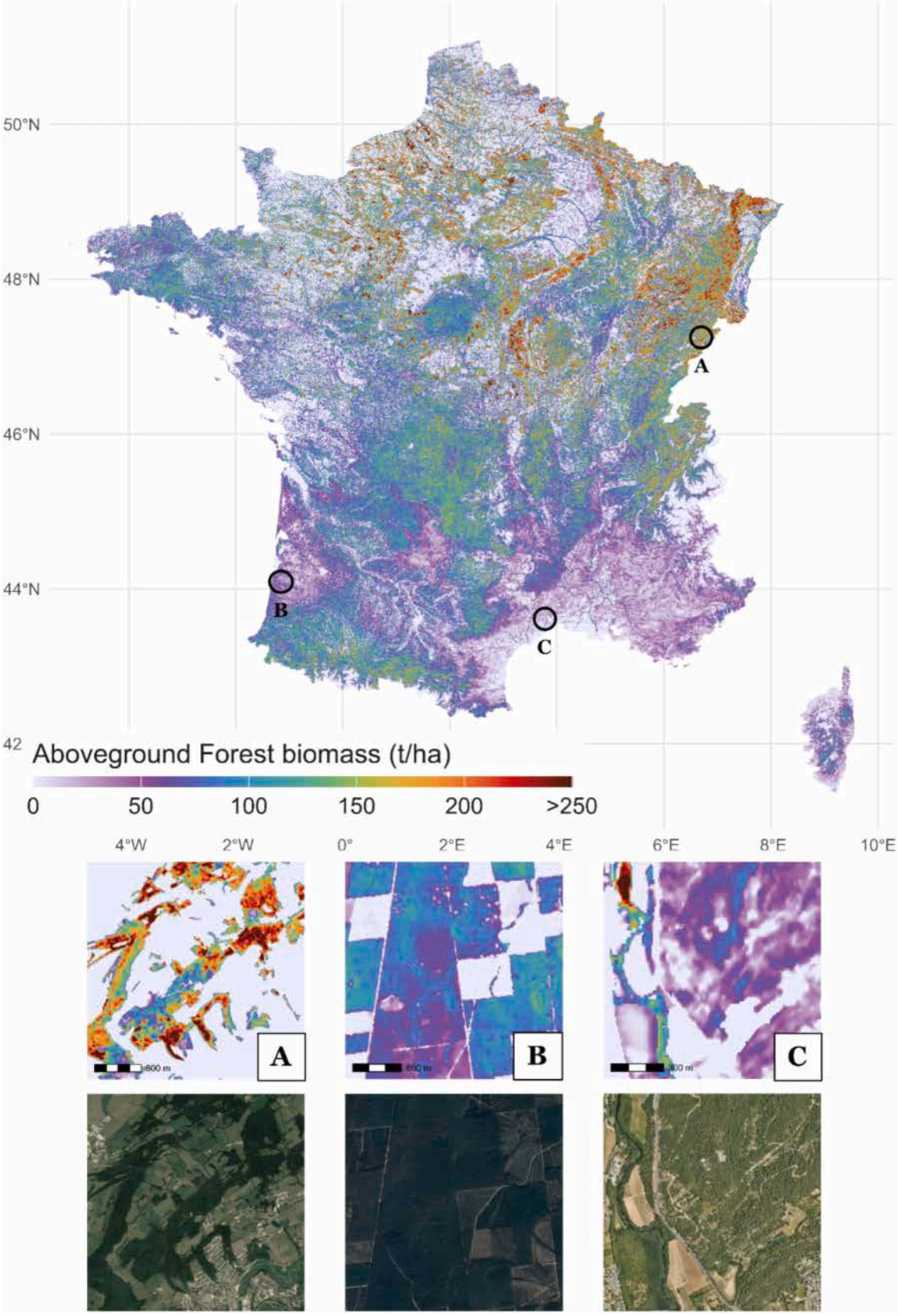

Fig. 5. Map of aboveground biomass (AGB) of forests in France. On the bottom, local snapshots showing the fine resolution (~10m) of the pixels. For better visualization, the data were resampled to 500m resolution for the national map.

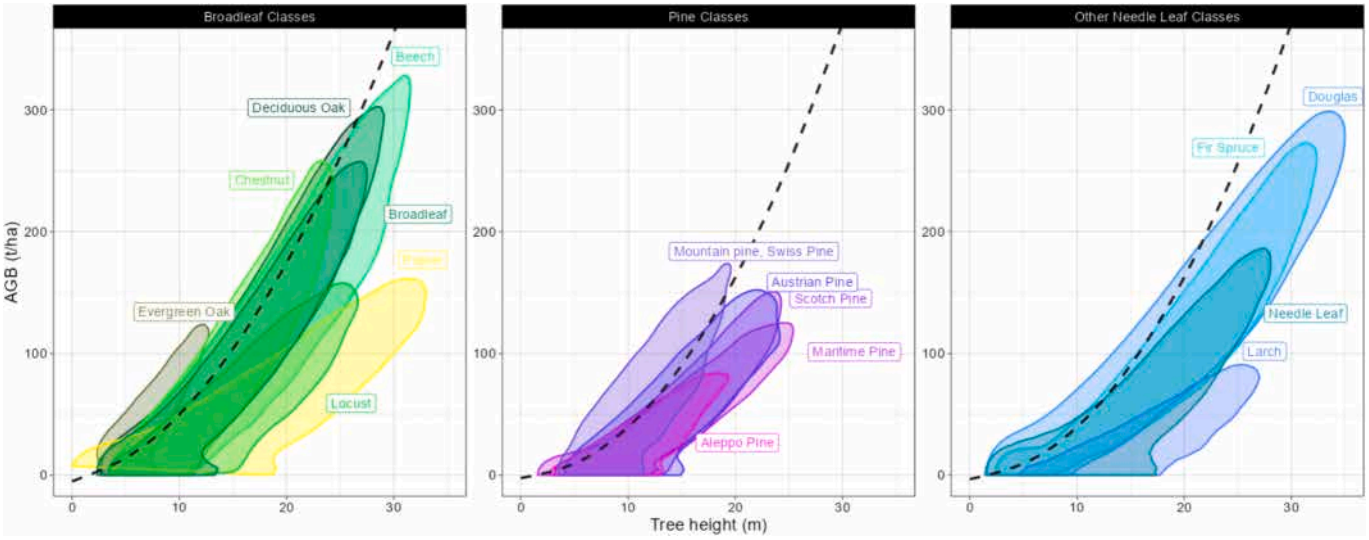

Figure 6. AGB (t/ha) and tree height (m) of forest classes. The dashed line corresponds to Schwartz et al (2023) direct estimation of AGB from tree height. Colored polygons correspond to the 90th percentile of AGB-Tree height density.

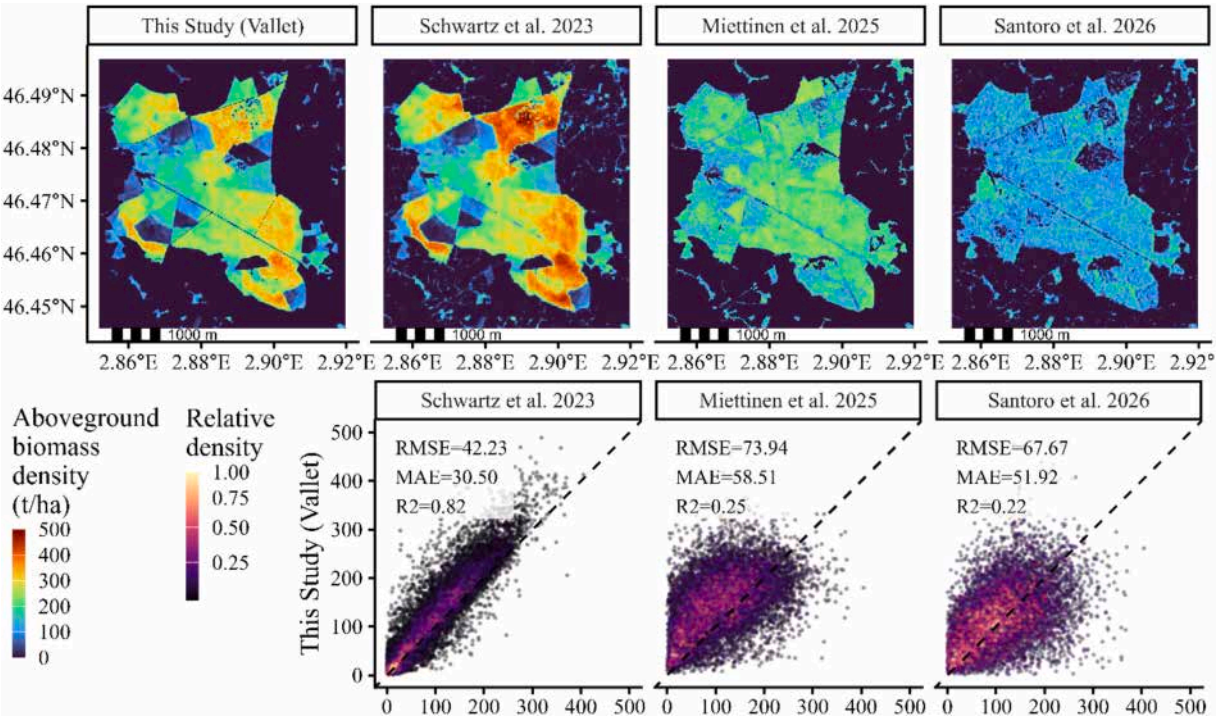

Figure 7. Intercomparison of the AGB map developed in this study with independent biomass products. Top row: zoom-in snapshots of aboveground biomass density (t/ha) over the same area for this study (Vallet), Schwartz et al (2023), Miettinen et al. (2025), and Santoro et al. (2026). All panels use the same colour scale to facilitate visual comparison. Bottom row: pixelwise comparison between our AGB map and each independent product using 100,000 co-located samples extracted over the common valid domain. The dashed line indicates the 1:1 relationship. Point colours represent relative sample density. Summary statistics (RMSE, MAE, R^2) are reported for each comparison.

temperature negatively affects predicted AGB, with a dAGB of 6.3 t/ha between mean annual temperatures of 10 °C and 15 °C. The occurrence of drought years following the 5 years of fire also acts as significant effect on the predicted AGB. A difference of 4.6 t/ha is observed between a burnt pixel that experienced a severe drought (SPEI=-2.5) and one that did not (SPEI=0).

Species traits also play an important role in predicted AGB. Bark thickness shows a positive effect with, for example, a dAGB of 6.6 t/ha between a trait value of 1 and 3. Note that the average predicted AGB around a bark thickness of 2 is lower. Ability to resprout has a strong positive effect on predicted AGB, with a dAGB of 18t/ha between trait values of 0 and 0.8. Conversely, serotiny does not have a major effect on predicted AGB. Surprisingly, dispersal distance negatively affects predicted AGB, showing a dAGB of 10.9 t/ha between trait values of 20 and 100. This can be explained on the one hand by the fact that the strategy associated with high dispersal distance corresponds to the landscape tolerator, a strategy that emerges over longer timescales and thus may not be captured within our 35-year study window. On the other hand, species with short dispersal distances are those with heavier seeds and higher mean intrinsic biomass than species with long dispersal

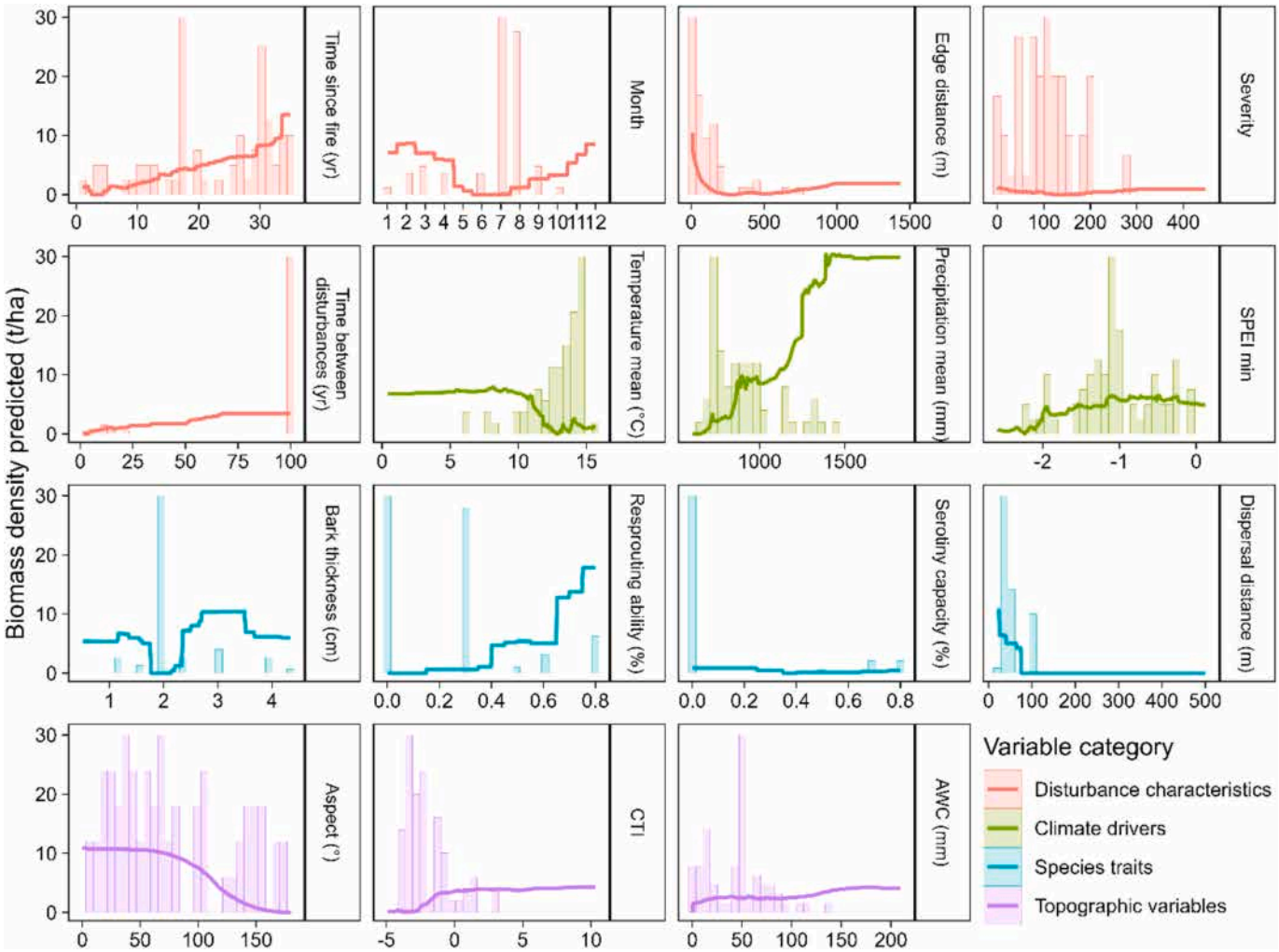

Fig 8. Partial (marginal) dependence curves of each explanatory variable on predicted aboveground biomass (AGB), derived from the Random Forest model. The bars indicate the frequency distribution of observed values for each predictor.

distances.

Topographical variables were finally identified as significant contributors on predicted AGB. Aspect has a significant negative effect, with north-facing slopes (0°) experiencing higher AGB (dAGB=10.3 t/ha) than the south-facing slopes (180°). In addition, CTI had a significant positive effect with pixels located on the valley floor (CTI=5) showing a higher AGB (dAGB=4.6 t/ha) than pixels on the ridgeline (CTI=-5). Finally, AWC shows a weak positive effect with a dAGB of 3.6 t/ha between an AWC of 0 and 100.

Our Random Forest model overall performed well in predicting AGB, with a correlation between observed and predicted values reaching an R^2 of 0.77 (Fig. A1) and an average magnitude or prediction errors of 17.8t/ha (RMSE).

3.3. Forest vulnerability mapping

Based on our random forest model, we could simulate a 40year time series of forest biomass post fire recovery accounting for climatic, species, and topographic drivers at the national level, from which we derived an objective and quantitative assessment of forest biomass vulnerability to fire at fine resolution (~10m) across France (Fig. 9). We observed from our results a higher biomass vulnerability in temperate forests, particularly in the northeast, with an average value of 3074 t.ha-1.yr and with values ranging from 2,000 to over 5,000 t.ha-1.yr. This is due first and foremost to the high level of exposure. Indeed, a high initial biomass value potentially leads to high vulnerability according to our index. However, it is also due to an overall lack of resistance and recovery of temperate systems to fire, further increasing vulnerability. Local variability can be observed in temperate forests. Valley bottoms and riverbanks show lower vulnerability, due to the greater resistance of forests to high temperatures during fires. Some forest areas, such as Scots pine forests, also show lower relative vulnerability, thanks in particular to their greater capacity to recover.

The Atlantic pine forest shows a much lower vulnerability than the temperate forest, with an average of 1368 t.ha-1.yr and most values ranging from 800 to 2000 t.ha.yr-1. This is due to the lower exposure and higher recovery capacity of maritime pines. Lastly, Mediterranean forests have a low vulnerability to wildfire with an average value of 731 t.ha-1.yr and most values between 400 and 1200 t.ha-1.yr. Evergreen oak forests, mainly in the west, show a high capacity for resistance and recovery, while Aleppo pine forest show a high capacity for recovery. Mediterranean forests have all the characteristics required for reduced vulnerability: relatively low exposure, high resistance, and strong recovery.

4. Discussion

4.1. Fire-induced carbon stock loss and recovery

As a first step forward and key result of our study, we could propose a

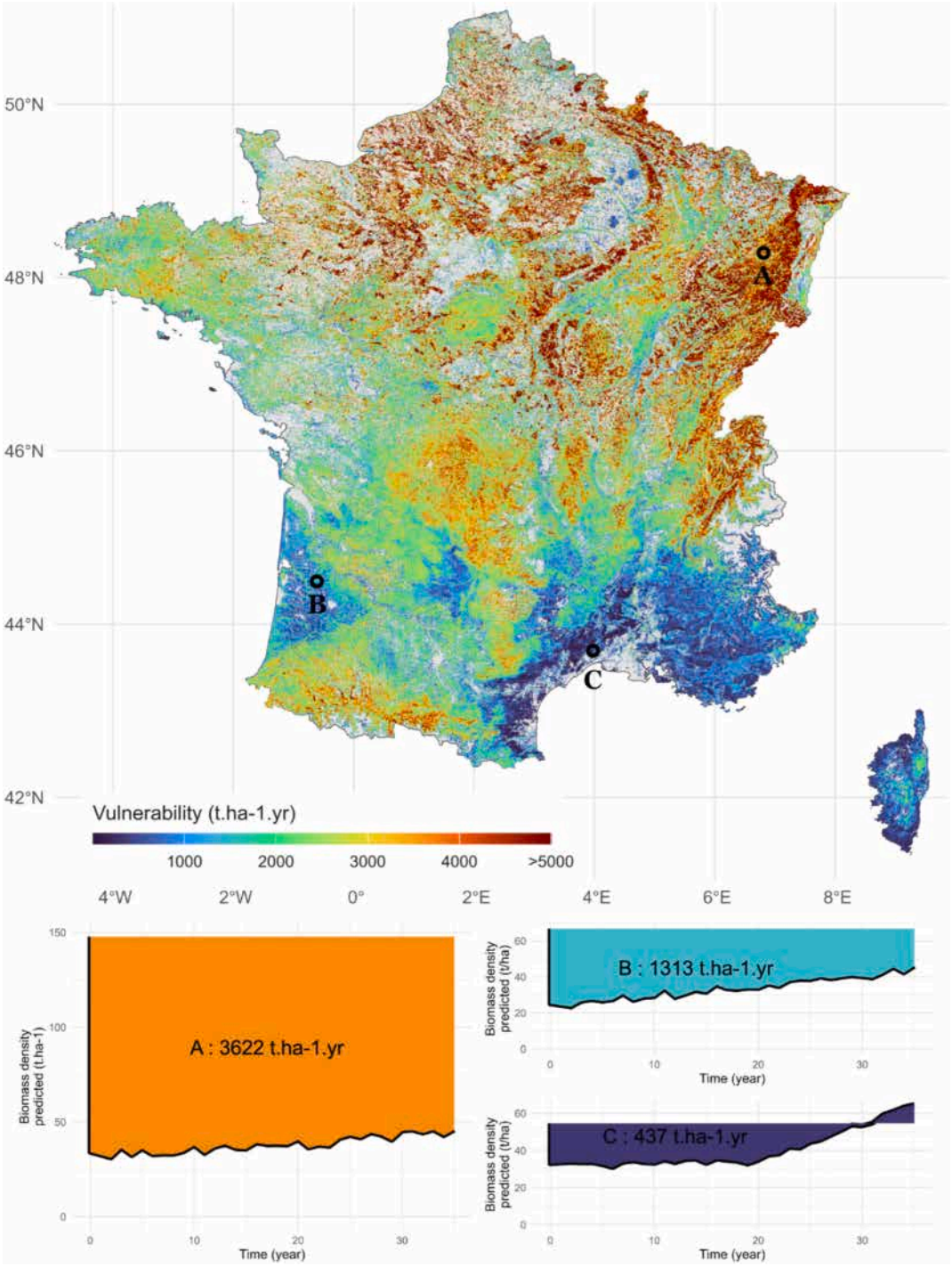

Figure 9. Forest fire vulnerability map. Values correspond to the absence of exposed biomass missing over 35 years. Vulnerability depends on forest exposure, resistance, and recovery. On the bottom, a representation of the vulnerability of three pixels (~10m) as an example. For better visualization, the data were resampled to 500m resolution for the national map.

revised aboveground carbon stock at the national territory level by leveraging the newly delivered GEDI-based tree height FORMS dataset (Schwartz et al., 2023). We estimated mean AGB of 32.0 t/ha for the mediterranean region, 53.4t/ha for the Atlantic forest and 110.9t/ha for the temperate forests, in accordance with the recent European forest inventory synthesis (Avitabile et al., 2024). Biomass mapping has long been challenging and leading to potential discrepancies (Avitabile & Camia, 2018), but the recently delivered tree height data could reduce this uncertainty and drastically increase the resolution. Yet, the various processing chains of GEDI data can lead to remaining uncertainties and discrepancies between global biomass datasets (Besic et al., 2024). Still, this new information offers the opportunity to better characterize wildfires by the exposure of assets in forest ecosystems. Based on this information, reports and media coverage of wildfire seasons can now be better contextualized in terms of disaster and biomass exposed to the disturbance. For instance, Vallet et al. (2023) could identify the distinctiveness of the extreme year 2022 not only based on its unusual burned area, but also by the averaged higher biomass exposed when affecting the northern part of the country, a relevant information, which could lie aside the cost (Meier et al., 2023) or population smoke

exposure (Xu et al., 2023) as an index of impacts to better characterize reported fire events.

More particularly, our study could reach a wildfire impact assessment at fine resolution by quantifying the territorial variability of forest resistance to wildfires and thus estimating the actual loss. We state here that for a similar biomass exposed, some more resistant species are less impacted. This resistance has long been recognized as primarily a function of a species' coping capacity from its biological traits (Dupire et al., 2019; Moris et al., 2022; Pausas, 2004; Rodman et al., 2021), although also affected by fire intensity (Trouve et al., 2021), climate (Cansler et al., 2024) and topographic conditions (Holik et al., 2025). We provided a data-driven estimate of carbon stock loss at the national level, based on exposed biomass and post-fire biomass remaining one year after the fire as an index of resistance. This information is hardly yet referenced in forest inventories, although of increasing concern as initiated for the US (Cansler et al., 2020). A key strength of our study is that it does not rely on *a priori* assumptions of resistance driven by plant traits but delivers a truly investigated index through the pre- and post-fire biomass. Species traits, used to classify our species rather than their taxon, appeared as a significant explanatory variable mostly through regeneration strategies (seeders or resprouters), thus strengthening our results that the observed biomass dynamic was related to their post-fire regeneration traits. We obtained a national map of carbon stock loss, correlated to pre-fire exposure as it is a fraction of the available biomass, but we could more particularly generate local variations driven by species functions, climate, and topographical features.

The main strength of our methodological development relies on the post-fire recovery assessment. A direct assessment would ideally require long-term observations of tree growth following a fire event to build a proper recovery, a target soon achievable with progresses in tree height time series delivery, yet covering only few years (Schwartz et al., 2025). Under the current absence of fine resolution time series of biomass dynamics, we relied on a space-for-time recovery assessment. We face the technical issue that temperate forests of northern France are only affected by significant fires during extreme fire weathers as during the recent years 2022 (Vallet et al., 2023), 2016 or 2003 (Curt & Frejaville, 2018), making the sample number discontinuous in time and insufficient for long-term reconstructions. We could compensate for this data gap by assembling species according to their fire response traits as a major tool in ecological modelling (Li et al., 2021). In turn, similar species could be used as a surrogate to reconstruct species biomass dynamic when historical fires were too sparse for a given species. We also faced the critical issue that direct assessments of recovery according to time since last fire could be affected by other disturbances and management practices as tree loss by logging (Ceccherini et al., 2020; Pellissier-Tanon et al., 2024). We filtered out these practices by using global tree loss data as detected by Hansen et al. (2013) or Senf and Seidl (2020b) to focus on fire disturbance only.

By removing other disturbances with the EU disturbance map, we removed any side effect of post-fire clear clutting. Yet, post fire forest plantation, along with restoration management practices (contour-felled log debris (CFD), log erosion barriers area (LEB) (Lucas-Borja et al., 2021; Moreira et al., 2012) might positively affect recovery rate or disturb soils and resprouting abilities (Jouy et al., 2025). Precise mapping and referencing of these management strategy implementations are however actually lacking. Surrogates for this information could integrate accessibility and topography for mapping forest management opportunities (Hengeveld et al., 2012; Neidermeier et al., 2023) as used in the EU fire risk mapping (Arrogante-Funes et al., 2024). This information has been refined at the national scale over France with forest accessibility (Dupire et al., 2015) and forest property (private or national) mapping (IFN) potentially driving managementy strategies. Yet, this information remains theoretically related to effective management plans and could bring more uncertainties than response function.

Based on this thorough method, we could reach substantially important quantitative assessment of post fire resistance and recovery for forest management policies and national carbon inventories including fire impact beyond emissions from combustion (Bowman et al., 2023). For instance, we could distinguish between fast recovery (within 35 years) mostly occurring in Mediterranean and Landes forests, and slower recovery in temperate forests, which often exceeds this period. This time frame of 35 years falls within the management planning strategy for carbon emission reduction plans to identify recovering and non-recovering areas, as keystone information for national carbon inventories and policy strategies (Cano et al., 2022; Chu et al., 2023). This recovery from past fires, with a decreasing trend in burned area since the end of the 1980's, might contribute to the currently observed increase in the growing stock of French forests (Bontemps et al., 2020), as evidenced for Canada through process-based modelling (Yue et al., 2013). A comparison between fire and logging impacts on carbon stock recovery should be assessed to better investigate how fires might more importantly jeopardize the forest carbon budget relative to commercial logging (Wilson et al., 2021).

4.2. Environmental drivers of forest vulnerability to fire

Our approach, using fine resolution datasets, could identify local modifiers of carbon stock vulnerability to fire, thus providing fine resolution impact assessment for post fire landscape management. As a dominant driver, regional climate based on mean annual temperature and precipitation revealed the higher post-fire biomass under colder and wetter conditions. This result is in agreement with previous results on post-fire recovery (Andrus et al., 2022; Baudena et al., 2020; Blanco-Rodríguez et al., 2023; Casady et al., 2010; Lippok et al., 2013; Spatola et al., 2023) and observed forest growth (Jevšenak et al., 2024; Pellissier-Tanon et al., 2024). Reduced precipitations during the summer season induces prolonged and earlier drought, which, combined with temperature-driven growth onset, highly constrains tree growth in mediterranean and temperate forests (Delpierre et al., 2016; Lempereur et al., 2017) Increasing drought and higher temperature from climate change might then alter the currently observed forest recovery (Tepley et al., 2017). In addition, we could identify that the interannual climate variations, and particularly drought during the 5 years after fires, might significantly alter post fire regeneration, (Harvey et al., 2016; Hérault & Piponiot, 2018; Meng et al., 2015; Viana-Soto et al., 2020), particularly for seeders whose germination (Chamorro et al., 2017) and seedling survival are affected by drought (Parra & Moreno, 2018). This results points out the potential enhanced effects of extreme years in promoting large fire events and limiting post-fire regrowth as a response to extreme and prolonged drought (Turco et al., 2017), so that climate change impacts on future fire risk should combine climate impact on fire hazard and subsequent climate affecting recovery (Akter et al., 2024).

We could also capture that the macroscale negative climate impacts on post-fire regrowth are potentially locally enhanced in south-facing slopes. This topographic position with more intense solar radiation and potential evapotranspiration affects forest functioning (Druel et al., 2025), seed production (Kemp et al., 2019), and post-fire regeneration through microclimatic heat and drought stress (Jung et al., 2023; Wooten et al., 2022). Shallow soils (ridge tops and low soil water retention potentials) were also identified as a significant driver affecting post-fire regeneration (Jouy et al., 2025), tree growth through earlier drought onset (Zribi et al., 2016). Assembled together, microscale topo-edaphic conditions appear as a keystone driver of overall recovery rate and post fire management (Chen et al., 2022; Ireland and Petropoulos,

2015; Johnstone et al., 2010; Nelson et al., 2014; Wittenberg et al., 2007). Under these local topo-edaphic conditions, drought features as duration or intensity have been shown to be more severe (Ruffault et al., 2013) and affect fire prone vegetation dynamic (Mouillot et al., 2005), and might be enhanced in the future with reduction in precipitation and increased temperatures (Ruffault et al., 2014).

We finally showed that fire types might play an important role in tree recovery. Fire severity, remotely sensed from the dNBR index, was not identified as a strong driver of biomass recovery in our study compared to previously reported investigations (Casady et al., 2010; Fernández-Guisuraga et al., 2022; Ireland and Petropoulos, 2015; Lv et al., 2025; Maringer et al., 2016; Meng et al., 2015; Viana-Soto et al., 2020). However we could confirm that shorter fire return interval and further distance to unburned patches significantly reduce post fire recovery as stated in local studies (Andrus et al., 2022; Braziunas et al., 2023; Díaz-Delgado et al., 2002; Harvey et al., 2016; Trang et al., 2023; Wittenberg et al., 2007). This result actually supports the vital attributes model (Noble & Slatyer, 1980) where a critical period between two successive fires is required for most seeder tree species to reach maturity and produce viable seeds for regeneration as Pinus halepensis (Rezgui et al., 2024), and a closer distance to the seed source (Christopoulou et al., 2014) favors regeneration and post fire vegetation dynamic (Mouillot et al., 2005). We could also point out that the season during which the fire occurs influences post-fire biomass growth. Early spring fires tend to enhance biomass regrowth (Kemp et al., 2019; Calvo et al., 1992), potentially with spring rainfalls allowing for enhanced seedling early-stage survival when compared to reduced seedling emergence during the summer dry season (Manela et al., 2022) Summer high temperatures have indeed been acknowledged to reduce seed germination (Tangney et al., 2020), as well as prolonged drought (Salesa et al., 2022), thus providing credit to out-of-season prescribed burning as a management tool (Fernandez-Guisuraga and Fernandes, 2024). However, more recent studies also suggest that out of season fires (i.e., outside the summer season) might alter their post fire seed germination adapted to the fire regime they have evolved with (Miller et al., 2021; Tangney et al., 2022).

4.3. Uncertainties and improvements

We could apply our space-for-time framework based on the achievement of a thoroughly visually checked Landsat-based burned area reconstruction since 1984 for 1762 fires larger than 20ha. Each fire was dated using the national fire database BDIFF, which covers the period from 2006 to the present over the whole national territory and since 1973 for the mediterranean part. We completed this database with 71 fires from text mining. This database is not exhaustive, and some small fires are still omitted. Systematic and automated Landsat processing are available, as for US (Hawbaker et al., 2020) or Europe (Senf & Seidl, 2020), but remain subject to uncertainties, including commission errors up to 14.6% and 41%, which could have compromised our analysis of recovery dynamic and add uncertainty in the distance to fire edges. In addition, Landsat-based burn dates cannot be provided and the uncertainty on the identification of burning years can reach up to 3 years in 77% of fire events (Senf and Seidl, 2020). This is a significant limitation, as our framework depends on accurate estimates of time since the last fire and includes the seasonal impact and post-fire drought as a driving factor requiring daily (or monthly) dating, and which appeared as significant contributors to the post-fire dynamics. We then relied on a semi-automated approach ensuring 0% commission error and precise daily timing based on official reports. Over 2006-2020, we captured 97.6% of fires larger than 50 ha, and 58.1% over 20ha, in the range of omission error from automated methods (19% to 32%). We could cover a time frame of 37 years, which might be too short for the full recovery of some species, but constitutes the most policy-relevant time-frame aligning with the Paris agreement goal to reach net-zero emissions by mid-century (Noon et al., 2021). We can deplore few significant fire events in the temperate sylvo-eco-region since 1984, inherent to the low fire hazard in this biome and small fires, leading to gaps in the post-fire recovery for some species. We balanced this data gap by using a trait-based approach and training the recovery of insufficiently burned species by their functionally most similar species. Further efforts should be devoted to automated or systematic referencing of fire events including fires smaller than 20ha (Kouachi et al., 2024; Majdalani et al., 2022). Processing landsat1-MSS for the 1974-1984 period could extend the recovery assessment by 10 years and better capture long-term recoveries only partially assessed in our study (Díaz-Delgado et al., 2004; Skakun et al., 2024).

Regarding biomass estimates, Schwartz et al. (2023) delivered a biomass information derived from tree height (FORMS) based on broadleaves and needle leaves tree height/biomass relationships over France. We developed here more species-specific relationship revised from Vallet et al. (2023) accounting for the varying wood densities across the mediterranean to temperate and Alpine bioclimate covering France. Uncertainties remain significant, but still below local or species-specific variabilities. To date, FORMS remains the most suitable tree height data for France compared to global datasets (Schwartz et al. (2023)). Ongoing progress in remote sensing would deliver in the near future fine resolution tree species mapping (Bolyn et al., 2022), better accounting for individual tree species with burned patches more accurately than our forest community-based approach. Similarly, we estimated species resistance by comparing unburned forests biomass to the biomass observed one year after fire events, thus only considering the fires of the year 2019 for tree height data only available for the year 2020 and extrapolated by our random forest algorithm for species not being affected during that year. The now available time series of GEDI data can provide yearly assessment of fire impacts on tree density and tree height (Guerra-Hernández et al., 2024), and in turn species resistance, that should be further analyzed to refine our findings.

The space-for-time substitution method used in our study for assessing forest carbon stocks resistance and recovery relies on the GEDI-based fine resolution tree height data recently released at the national level in France for the year 2020 (Schwartz et al., 2023). Alternative strategies for space-for-time forest recovery analysis may rely on forest inventories (Kashian et al., 2013; Palviainen et al., 2020; Wilson et al., 2021), using few plots per selected fire. French National Forest Inventory provides tree height and volume over 31600 plots at 1km resolution over forested areas (IGN, 2018). Using these data could have been an alternative methodological approach as performed by Pellissier-Tanon et al. (2024) for northern France, although considerably reducing the number of environmental conditions that would have altered the robustness of the identification of local drivers affecting post-fire biomass dynamics. Other alternative approaches performed dynamic post-fire recovery on tree height and biomass leveraging GEDI data (only available since 2016) and interpolating backwards in time this information with Landsat composite-GEDI relationships reaching R^2 varying between 0.51 and 0.74 and RMSE varying between 24% and 36% (Turubanova et al., 2023; Viana-Soto et al., 2022). We based our space for time analysis with a constant climate as some studies illustrate low temporal changes in tree growth change over the last decades in Europe. This was illustrated for Scot Pine over Europe and France by

Pretzsch et al. (2023), although some other studies could conclude on a 20%-30% decrease for Beech forests productivity (Martinez Del Castillo et al., 2022). Similarly, at the national level, Hertzog et al. (2025) could actually identify a turning in forest productivity over the 1978-2023 period, based on the national forest inventory, with stable to quadratic trends over most of the temperate forests, and linear decline by 20 to 30% over the mediterranean climate. This decline can be related to an earlier drought onset observed over the region (Ruffault et al., 2013) and controlling tree basal area increment (Lempereur et al., 2017), although compensated by earlier start of the growing season with higher winter temperatures. Regarding these divergent species responses and mechanistic processes hardly integrated in statistical models, we thus considered the climate gradient response only, and skipped this complex climate responses varying across time. We acknowledge the potentially weak predictive value of this space for time approach as stated by Perret et al. (2024), that could be refined in further studies.

4.4. Applications and perspectives

Our study providing territorial-scale fire effects on tree biomass loss and recovery could finally pave the way for assessing economic losses from timber prices (Sweeney et al., 2023) or animal biodiversity based on habitat description based on tree height (Kebrle et al., 2021; Komlós et al., 2024) and landscape pattern (Bonthoux et al., 2018; Brotons et al., 2005). Combined with fine resolution fire hazard mapping from statistical (Pimont et al., 2021; Trucchia et al., 2023) or process-based fire spread modeling (Salis et al., 2023) would provide the full scheme for fire risk assessment (Chuvieco et al., 2023). Accounting for post-fire dead tree dynamics and soil carbon should be further considered for a full carbon vulnerability assessment. For example, Reilly et al. (2023) illustrated the delayed post fire mortality from dNBR time series analysis, and Putman et al. (2018) could provide standing dead tree structural loss, two key components not accounted for in our approach. Soil carbon combustion and recovery remain the main challenge to date (Cheng et al., 2023), yet potentially contributing significantly to fire emissions in temperate forest as evidenced by Vallet et al. (2025) over France. Hardly detected from remote sensing over large areas, combining remote sensing, field observations and modelling approaches (Hu et al., 2023) should be a targeted research opportunity, including peatlands depth loss during fire events and recovery from fine resolution airborne lidar (Chasmer et al., 2017).

Our modeling framework, providing forest biomass as a function of time, includes the key drivers of fire season and distance to fire edge (that increase with fire size), with enhanced recovery for spring and small fires. These results constitute a keystone information available at the national level demonstrating how smaller fires occurring outside the natural summer fire season could sustain higher forest resilience. This would support the current directives and EU policies in promoting integrated fire management (Oliveras Menor et al., 2025) and nature-based solution (Domingos et al., 2025) for limiting fire hazards and its impacts (Plana et al., 2024), with, among others, prescribed burning proposed as an efficient management tool (Fernandes, 2015; Fernandes et al., 2013; Hunter & Robles, 2020; Pacheco & Claro, 2021). These fires are typically conducted in early spring, when fire weather conditions are less hazardous, preventing escaped fires over large areas (Neidermeier et al., 2023). Delivering this knowledge about forest resilience to fire would help forest stakeholders and societies to better acknowledge the benefits of prescribed burning beyond the fear trap (Castellnou et al., 2019) and toward a better societal awareness (Kreuter et al., 2025) removing acceptance barriers currently encountered (Smithwick et al., 2024).

Combined with spatially-explicit process-based models used to assess prescribed fire impacts on subsequent wildfire hazard (Piñol et al., 2005), our framework can quantitatively assess their effects on carbon stock loss and recovery compared to wildfire. This could be used as an efficient tool guiding future policies under climate change and subsequent forest species change (Dyderski et al., 2018) or fire regime shifts (Galizia et al., 2023).

Our mapping of forest carbon stock vulnerability to fires finally questions future strategies for targeted fire management and protection zones. Protected areas experience more natural fire ignitions and burned area (Arellano-del-Verbo et al., 2023; Resco De Dios et al., 2025a,b; Cardil et al., 2026), and fire exclusion zones tend to promote fuel build up and degrade resistance and resilience forest species communities (Hagmann et al., 2022), thus jeopardizing these criteria for an inclusion in the decision process for new or readjusted protected areas. Forest carbon storage and ecological structure based on fine resolution tree height and biomass (Liang et al., 2023), associated to their vulnerability to fires as provided by our study could play a significant role in revealing current gaps and new opportunities for protected areas (Mouillot et al., 2024).

5. Conclusion

We leveraged newly delivered Landsat-based fire history reconstruction over the 1984-2020 period and fine resolution tree height datasets to propose an objective and data-driven quantification of carbon loss, and recovery in forested ecosystems over the France national territory. By combining biomass assessment from tree height, local forest inventories for the year 2020 and forest species similarities from fire-related functional traits, we could propose a space-for-time methodology to reconstruct biomass dynamics since the last fire. Our results provide a quantitative high-resolution map of forest vulnerability to wildfires, illustrating national-scale heterogeneity that can nuance conclusions based solely on annual burned area extremes. We also identified local constraints as slope orientation, soil available water capacity and local climate or post fire drought events, as well as fire types and seasonality, which are key drivers of aboveground forest carbon stock vulnerability. These results bring a keystone fine resolution information for local decision making on forest protection, firefighting strategies or implementation of new strategic policies toward integrated fire management strategies, including prescribed burnings replacing summer large fires by smaller spring fires enhancing forest recovery.

CRediT authorship contribution statement

Lilian Vallet: Writing – review & editing, Writing – original draft, Visualization, Methodology, Investigation, Formal analysis, Data curation, Conceptualization. **Florent Mouillot:** Writing – review & editing, Writing – original draft, Supervision, Methodology, Funding acquisition, Conceptualization.

Declaration of competing interest

The authors declare that they have no known competing financial interests or personal relationships that could have appeared to influence the work reported in this paper.

Acknowledgment

This work was supported by the French Environment and Energy Management Agency (ADEME) and the FirEUrisk H2020 project (grant agreement no. 101003890), providing the phD grant to Lilian Vallet, along with the French national support of ANR FIRE-LANDES (ANR-23-CE02-0031) and QWERTY (ANR-25-PEFO-0008), the EU MSCA Staff Exchange FIRE-ADAPT project (no. 101086416), and the OSU OREME providing long-term support for fire observation.

Appendix A. Appendix

Table A1
: Functional trait values used in the post-fire biomass estimation model: BA: Bark thickness, RA: Resprouting ability, SC: Serotiny capacity, SD :Seed dispersal. 1: (Restor, 2026), 2:(Yilmaz et al., 2021), 3:(Schwörer et al., 2014), 4:(Tavşanoğlu & Pausas, 2018), 5: (Catry et al., 2013), 6:(Kühn et al., 2004), 7:(Rosell, 2016), 8:(Lojo et al., 2021), 9:(Pausas et al., 2016), 10:(Stone, 2009), 11:(Saulino et al., 2023), 12:(He et al., 2012), 13:(Wirth & Lichstein, 2009), 14:(Pellegrini et al., 2017), 15: (Chiriacò et al., 2013), 16:(Mauri et al., 2022)

Forest class	*Bark thickness*	*Resprouting ability*	*Serotiny capacity*	*Dispersal distance*	*References*
BROADLEAF	2	0,3	0	30	
Deciduous Oak	1,1	0,6	0	30	BA : 1,2 ; RA : 3,4 SC : 4 ; SD : 3
Evergreen Oak	3	0,8	0	30	BA : 4,5,6,7 ; RA : 4 SC : 4 ; SD : 3
Beech	2,4	0,7	0	30	BA : 8 ; RA : 3,4 SC : 4 ; SD : 3
Chestnut	1,2	0,5	0	20	BA : 4,5 ; RA : 4 SC : 4 ; SD : 3
Poplar	0,5	0,8	0	500	BA : 1 ; RA : 9 SC : 9 ; SD : 3
Locust	2	0	0,5	50	BA : 10 ; RA : 10,11 SC : 4 ; SD : 3
NEEDLE LEAF	2	0	0,5	50	
PINES					
Maritime Pine	4	0	0,7	100	BA : 4,5,6,7,12 ; RA : 4 SC : 4 ; SD : 3
Scotch Pine	4,34	0	0	100	BA : 4,7,12 ; RA : 3,4 SC : 4 ; SD : 3,13
Austrian Pine	1,5	0	0	100	BA : 12 ; RA : 3 SC : 4 ; SD : 3
Aleppo Pine	2,3	0	0,8	100	BA : 4,12 ; RA : 4 SC : 4 ; SD : 3
Mountain pine, Swiss Pine	1	0	0,5	30	BA : 12 ; RA : 4 SC : 4 ; SD : 3
OTHER NEEDLE LEAF					
Fir Spruce	1	0	0	100	BA : 7,12 ; RA : 3 SC : 4 ; SD : 3
Larch	2	0	0	100	BA : 14 ; RA : 3 SC : 4 ; SD : 3
Douglas	3	0	0	100	BA : 7,12,15 ; RA : 12 SC : 16 ; SD : 13
Needle Leaf	2	0	0	100	
MIXED FOREST	2	0	0	50	

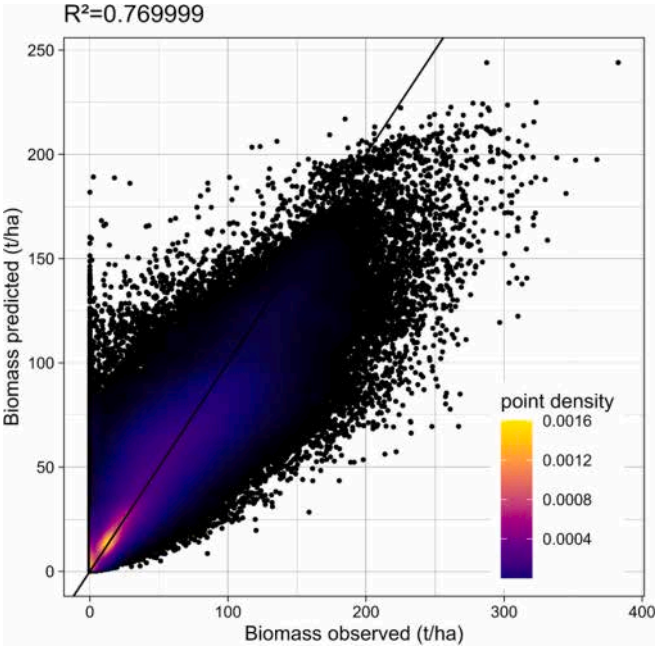

Fig. A1. Random forest predicted biomass and observed biomass, ie AGB map of 2020. These data correspond to the 10% of pixels not used to construct the random forest.

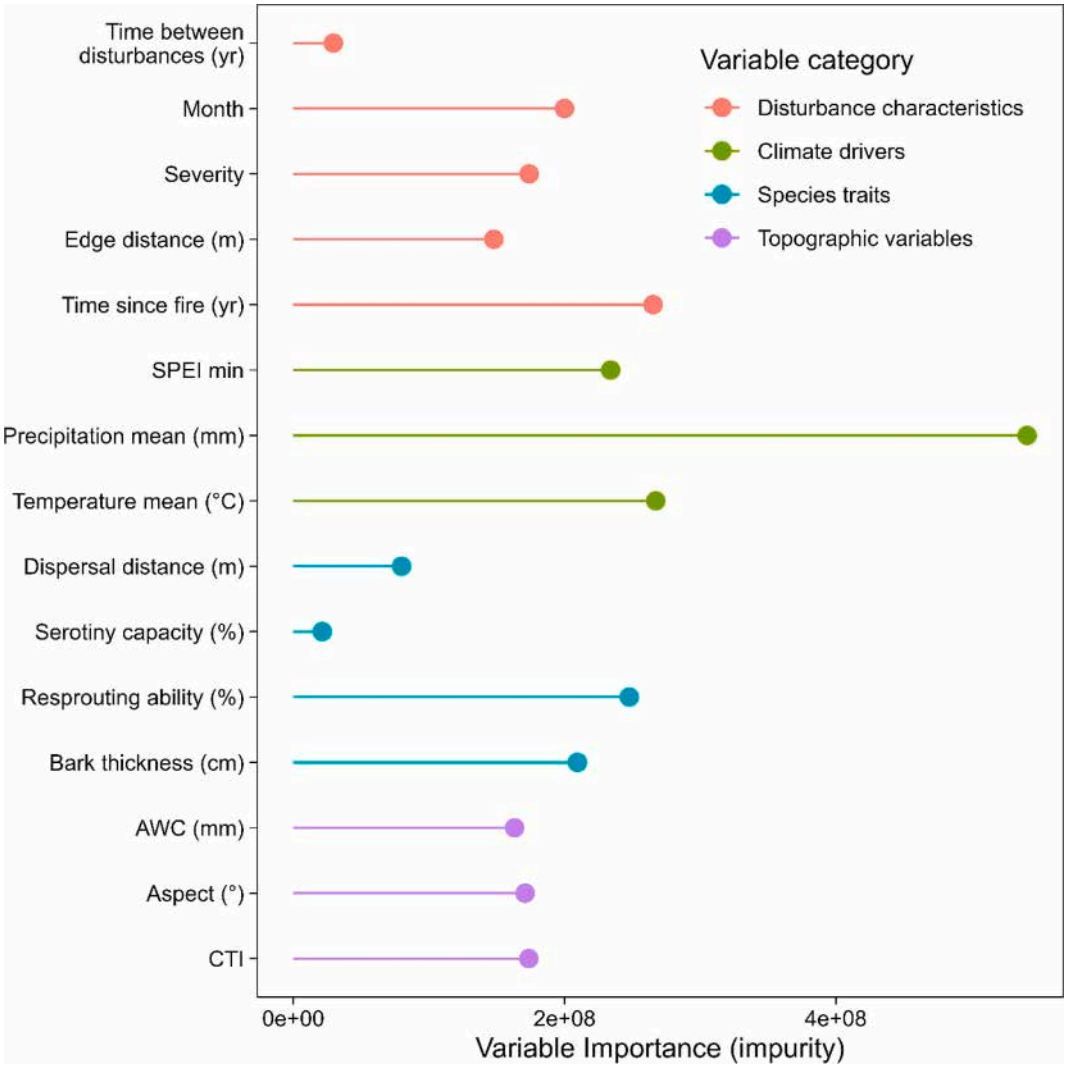

Fig. A2. Relative importance of predictor variables derived from the Random Forest model. Relative contribution of each predictor to the model's accuracy, expressed as the mean decrease in impurity. Variables are grouped by category : disturbance characteristics (red), climate drivers (green), species traits (blue), and topographic variables (purple). The horizontal line length reflects each variable's relative importance.

Data availability

Data will be made available on request.

References

Abatzoglou, J.T., Williams, A.P., Boschetti, L., Zubkova, M., Kolden, C.A., 2018. Global patterns of interannual climate-fire relationships. Glob. Chang. Biol. 24 (11), 5164–5175. https://doi.org/10.1111/gcb.14405.

Akter, S., Dube, O.P., Villagra, P., Mockrin, M., Taylor, S., Roald, L.A., Di Giuseppe, F., Wu, C., Fernandes, P.M., Rouet-Leduc, J., 2024. Fire risk in a warming world. One Earth 7 (6), 927–931. https://doi.org/10.1016/j.oneear.2024.05.020.

Amador-Cruz, F., Figueroa-Rangel, B.L., Olvera-Vargas, M., Mendoza, M.E., 2021. A systematic review on the definition, criteria, indicators, methods and applications behind the Ecological Value term. Ecol. Indic. 129, 107856. https://doi.org/10.1016/j.ecolind.2021.107856.

Andrus, R.A., Droske, C.A., Franz, M.C., Hudak, A.T., Lentile, L.B., Lewis, S.A., Morgan, P., Robichaud, P.R., Meddens, A.J.H., 2022. Spatial and temporal drivers of post-fire tree establishment and height growth in a managed forest landscape. Fire Ecol. 18 (1), 29. https://doi.org/10.1186/s42408-022-00153-4.

Angeler, D.G., Allen, C.R., 2016. Quantifying resilience. J. Appl. Ecol. 53 (3), 617–624. https://doi.org/10.1111/1365-2664.12649.

Archibald, S., Hempson, G.P., Lehmann, C., 2019. A unified framework for plant life history strategies shaped by fire and herbivory. New Phytol 224, 1490–1503. https://doi.org/10.1111/nph15986.

Arellano-del-Verbo, G., Urbieta, I.R., Moreno, J.M., 2023. Large-Fire Ignitions Are Higher in Protected Areas than Outside Them in West-Central Spain. Fire 6 (1), 28. https://doi.org/10.3390/fire6010028.

Arrogante-Funes, F., Florent, Mouillot, Moreira, B., Aguado, I., Chuvieco, E., 2024. Mapping and assessment of ecological vulnerability to wildfires in Europe. Fire Ecol. 20 (1), 98.

Aven, T., 2011. On some recent definitions and analysis framework for risk, vulnerability, and resilience. Risk Analysis 31, 515–522. https://doi.org/10.1111/j.1539-6924.2010.01528.x.

Avitabile, V., Camia, A., 2018. An assessment of forest biomass maps in Europe using harmonized national statistics and inventory plots. For. Ecol. Manag. 409, 489–498. https://doi.org/10.1016/j.foreco.2017.11.047.

Avitabile, V., Pilli, R., Migliavacca, M., Duveiller, G., Camia, A., Blujdea, V., Adolt, R., Alberdi, I., Barreiro, S., Bender, S., Borota, D., Bosela, M., Bouriaud, O., Breidenbach, J., Cañellas, I., Čavlović, J., Colin, A., Di Cosmo, L., Donis, J., Mubareka, S., 2024. Harmonised statistics and maps of forest biomass and increment in Europe. Sci. Data 11 (1), 274. https://doi.org/10.1038/s41597-023-02868-8.

Bastarrika, A., Alvarado, M., Artano, K., Martinez, M., Mesanza, A., Torre, L., Ramo, R., Chuvieco, E., 2014. BAMS: A Tool for Supervised Burned Area Mapping Using Landsat Data. Remote Sens. 6, 12360–12380. https://doi.org/10.3390/rs61212360.

Baudena, M., Santana, V.M., Baeza, M.J., Bautista, S., Eppinga, M.B., Hemerik, L., Garcia Mayor, A., Rodriguez, F., Valdecantos, A., Vallejo, V.R., Vasques, A., Rietkerk, M., 2020. Increased aridity drives post-fire recovery of Mediterranean forests towards open shrublands. New Phytol. 225 (4), 1500–1515. https://doi.org/10.1111/nph.16252.

BDIFF. https://bdiff.agriculture.gouv.fr/, 2026 last access: 8 March 2023.

Beguería, S., Vicente-Serrano, S.M., Reig, F., Latorre, B., 2014. Standardized precipitation evapotranspiration index (SPEI) revisited: parameter fitting,

evapotranspiration models, tools, datasets and drought monitoring. Int. J. Climatol. 34, 3001–3023. https://doi.org/10.1002/joc.3887.
Belgiu, M., Drăguţ, L., 2016. Random forest in remote sensing: A review of applications and future directions. ISPRS J. Photogramm. Remote Sens. 114, 24–31. https://doi.org/10.1016/j.isprsjprs.2016.01.011.
Berchtold (née Bach), C., Viegas, D., G. Borges, J., Vallim, D., Chandramouli, K., Plana Bach, E., Núria, P., Brunet-Navarro, P., Górriz Mifsud, E., Kalapodis, Dr. N., Sakkas, G., Gonzalez-Aguilera, D., Chuvieco, E., Pausas, J., Doerr, S. H., Almeida, P. M., Thonicke, K., & Eftychidis, G, 2025. An Integrated Wildfire Risk Management Strategy for the. Developing resilient landscapes and safer communities, EU. https://doi.org/10.5281/ZENODO.15525837.
Besic, N., Picard, N., Vega, C., Hertzog, L., Renaud, J.-P., Fogel, F., Pellissier-Tanon, A., Destouet, G., Planells-Rodriguez, M., Ciais, P., 2024. Remote sensing-based high-resolution mapping of the forest canopy height: Some models are useful, but might they be even more if combined? https://doi.org/10.5194/gmd-2024-95.
Blanco-Rodríguez, M.Á., Ameztegui, A., Gelabert, P., Rodrigues, M., Coll, L., 2023. Short-term recovery of post-fire vegetation is primarily limited by drought in Mediterranean forest ecosystems. Fire Ecol. 19 (1), 68. https://doi.org/10.1186/s42408-023-00228-w.
Bolyn, C., Lejeune, P., Michez, A., Latte, N., 2022. Mapping tree species proportions from satellite imagery using spectral–spatial deep learning. Remote Sens. Environ. 280, 113205. https://doi.org/10.1016/j.rse.2022.113205.
Bončina, A., Klopčič, M., Trifković, V., Ficko, A., Simončič, P., 2023. Tree and stand growth differ among soil classes in semi-natural forests in central Europe. CATENA 222, 106854. https://doi.org/10.1016/j.catena.2022.106854.
Bontemps, J.-D., Denardou, A., Hervé, J.-C., Bir, J., Dupouey, J.-L., 2020. Unprecedented pluri-decennial increase in the growing stock of French forests is persistent and dominated by private broadleaved forests. Ann. For. Sci. 77 (4), 98. https://doi.org/10.1007/s13595-020-01003-6.
Bonthoux, S., Lefèvre, S., Herrault, P.-A., Sheeren, D., 2018. Spatial and Temporal Dependency of NDVI Satellite Imagery in Predicting Bird Diversity over France. Remote Sens. 10, 1136. https://doi.org/10.3390/rs10071136.
Bowman, D.M., Williamson, G.J., Ndalila, M., Roxburgh, S.H., Suitor, S., Keenan, R.J., 2023. Wildfire national carbon accounting: How natural and anthropogenic landscape fires emissions are treated in the 2020 Australian government greenhouse gas accounts report to the UNFCCC. Carbon Balance and Management 18 (1), 14. https://doi.org/10.1186/s13021-023-00231-3.
Braziunas, K.H., Kiel, N.G., Turner, M.G., 2023. Less fuel for the next fire? Short-interval fire delays forest recovery and interacting drivers amplify effects. Ecology 104 (6), e4042. https://doi.org/10.1002/ecy.4042.
Brotons, L., Herrando, S., Martin, J.-L., 2005. Bird assemblages in forest fragments within Mediterranean mosaics created by wild fires. Landsc. Ecol. 19 (6), 663–675. https://doi.org/10.1007/s10980-005-0165-2.
Calvo, L., Tarrega, R., Luis, E., Marcos, E., 1992. Differences in Vegetal Regeneration by Effects of Spring and Summer Fires in Quercus Pyrenaica Forests. In: Teller, A., Mathy, P., Jeffers, J.N.R. (Eds.), Responses of Forest Ecosystems to Environmental Changes. Springer, Netherlands, pp. 855–857. https://doi.org/10.1007/978-94-011-2866-7_194.
Cano, I.M., Shevliakova, E., Malyshev, S., John, J.G., Yu, Y., Smith, B., Pacala, S.W., 2022. Abrupt loss and uncertain recovery from fires of Amazon forests under low climate mitigation scenarios. Proc. Natl. Acad. Sci. 119 (52), e2203200119. https://doi.org/10.1073/pnas.2203200119.
Cansler, C.A., Hood, S.M., Varner, J.M., Van Mantgem, P.J., Agne, M.C., Andrus, R.A., Ayres, M.P., Ayres, B.D., Bakker, J.D., Battaglia, M.A., Bentz, B.J., Breece, C.R., Brown, J.K., Cluck, D.R., Coleman, T.W., Corace, R.G., Covington, W.W., Cram, D.S., Cronan, J.B., Wright, M.C., 2020. The Fire and Tree Mortality Database, for empirical modeling of individual tree mortality after fire. Sci. Data 7 (1), 194. https://doi.org/10.1038/s41597-020-0522-7.
Cansler, C.A., Wright, M.C., Van Mantgem, P.J., Shearman, T.M., Varner, J.M., Hood, S. M., 2024. Drought before fire increases tree mortality after fire. Ecosphere 15 (12), e70083. https://doi.org/10.1002/ecs2.70083.
Cardil, A., Mola-Yudego, B., Blázquez-Casado, Á., González-Olabarria, J.R., 2019. Fire and burn severity assessment: Calibration of Relative Differenced Normalized Burn Ratio (RdNBR) with field data. J. Environ. Manag. 235, 342–349. https://doi.org/10.1016/j.jenvman.2019.01.077.
Cardil, A., Rodrigues, M., Ascoli, D., Ortega, M., Quiñones, T., Erdozain, M., Menor, I.O., Spadoni, G.L., Ramírez, J., Molina, J.R., Mouillot, F., Silva, C.A., Mohan, M., Martínez-Bentué, C., de-Miguel S., 2026. Protected areas influence fire regimes globally. J. Environ. Manag. 398, 128285.
Casady, G.M., Van Leeuwen, W.J.D., Marsh, S.E., 2010. Evaluating Post-wildfire Vegetation Regeneration as a Response to Multiple Environmental Determinants. Environ. Model. Assess. 15 (5), 295–307. https://doi.org/10.1007/s10666-009-9210-x.
Castellnou, M., Prat-Guitart, N., Arilla, E., Larranaga, A., Nebot, E., Castellarnau, X., Vendrell, J., Pallas, J., Herrera, J., Monturiol, M., Cespedes, J., Pagès, J., Gallardo, C., Miralles, M., 2019. Empowering strategic decision-making for wildfire management: avoiding the fear trap and creating a resilient landscape. Fire Ecology 15, 31. https://doi.org/10.1186/s42408-019-0048-6.
Ceccherini, G., Duveiller, G., Grassi, G., Lemoine, G., Avitabile, V., Pilli, R., Cescatti, A., 2020. Abrupt increase in harvested forest area over Europe after 2015. Nature 583 (7814), 72–77. https://doi.org/10.1038/s41586-020-2438-y.
Celebrezze, J.V., Franz, M.C., Andrus, R.A., Stahl, A.T., Steen-Adams, M., Meddens, A.J. H., 2024. A fast spectral recovery does not necessarily indicate post-fire forest recovery. Fire Ecol. 20 (1), 54. https://doi.org/10.1186/s42408-024-00288-6.
Chamorro, D., Luna, B., Ourcival, J.-M., Kavgacı, A., Sirca, C., Mouillot, F., Arianoutsou, M., Moreno, J.M., 2017. Germination sensitivity to water stress in four shrubby species across the Mediterranean Basin. Plant Biol. 19 (1), 23–31. https://doi.org/10.1111/plb.12450.
Chasmer, L.E., Hopkinson, C.D., Petrone, R.M., Sitar, M., 2017. Using Multitemporal and Multispectral Airborne Lidar to Assess Depth of Peat Loss and Correspondence With a New Active Normalized Burn Ratio for Wildfires. Geophys. Res. Lett. 44. https://doi.org/10.1002/2017GL075488.
Chen, X., Chen, W., Xu, M., 2022. Remote-Sensing Monitoring of Postfire Vegetation Dynamics in the Greater Hinggan Mountain Range Based on Long Time-Series Data: Analysis of the Effects of Six Topographic and Climatic Factors. Remote Sens. 14, 2958. https://doi.org/10.3390/rs14132958.
Cheng, Y., Luo, P., Yang, H., Li, H., Luo, C., Jia, H., Huang, Y., 2023. Fire effects on soil carbon cycling pools in forest ecosystems: A global meta-analysis. Sci. Total Environ. 895, 165001. https://doi.org/10.1016/j.scitotenv.2023.165001.
Chiriacò, M.V., Perugini, L., Cimini, D., D'Amato, E., Valentini, R., Bovio, G., Corona, P., Barbati, A., 2013. Comparison of approaches for reporting forest fire-related biomass loss and greenhouse gas emissions in southern Europe. Int. J. Wildland Fire 22, 730. https://doi.org/10.1071/WF12011.
Christopoulou, A., Fyllas, N.M., Andriopoulos, P., Koutsias, N., Dimitrakopoulos, P.G., Arianoutsou, M., 2014. Post-fire regeneration patterns of Pinus nigra in a recently burned area in Mount Taygetos, Southern Greece: The role of unburned forest patches. For. Ecol. Manag. 327, 148–156. https://doi.org/10.1016/j.foreco.2014.05.006.
Chu, L., Grafton, R.Q., Nelson, H., 2023. Accounting for forest fire risks: Global insights for climate change mitigation. Mitig. Adapt. Strateg. Glob. Chang. 28 (8), 48. https://doi.org/10.1007/s11027-023-10087-0.
Chuvieco, E., Mouillot, F., Van Der Werf, G.R., San Miguel, J., Tanase, M., Koutsias, N., García, M., Yebra, M., Padilla, M., Gitas, I., Heil, A., Hawbaker, T.J., Giglio, L., 2019. Historical background and current developments for mapping burned area from satellite Earth observation. Remote Sens. Environ. 225, 45–64. https://doi.org/10.1016/j.rse.2019.02.013.
Chuvieco, E., Yebra, M., Martino, S., Thonicke, K., Gómez-Giménez, M., San-Miguel, J., Oom, D., Velea, R., Mouillot, F., Molina, J.R., Miranda, A.I., Lopes, D., Salis, M., Bugaric, M., Sofiev, M., Kadantsev, E., Gitas, I.Z., Stavrakoudis, D., Eftychidis, G., Bar-Massada, A., Neidermeier, A., Pampanoni, V., Pettinari, M.L., Arrogante-Funes, F., Ochoa, C., Moreira, B., Viegas, D., 2023. Towards an Integrated Approach to Wildfire Risk Assessment: When. Where, What and How May the Landscapes Burn, Fire 6, 215. https://doi.org/10.3390/fire6050215.
Copernicus Land Monitoring Service. https://land.copernicus.eu/pan-european/high-resolution-layers/forests/tree-cover-density/status-maps/tree-cover-density-2018, 2026 last access: 15 March 2023.
Coppola, D.P., 2015. Risk and vulnerability. In: Coppola, D.P. (Ed.), Introduction to International Disaster Management. Butterworth-Heinemann, Third Edition. https://doi.org/10.1016/B978-0-12-801477-6.00003-4.
Costa, J.M., Heleno, R.H., Lopes, P., Ramos, J.A., Marchante, E., Vargas, P., Timóteo, S., 2025. Seed dispersal as a backup system to resprouting and seeding during post-fire regeneration. Ann. Bot. mcaf230. https://doi.org/10.1093/aob/mcaf230.
Curt, T., Frejaville, T., 2018. Wildfire Policy in Mediterranean France: How Far is it Efficient and Sustainable? Risk Anal. 38 (3), 472–488. https://doi.org/10.1111/risa.12855.
Dakos, V., Kéfi, S., 2022. Ecological resilience: What to measure and how. Environ. Res. Lett. 17 (4), 043003. https://doi.org/10.1088/1748-9326/ac5767.
Delpierre, N., Berveiller, D., Granda, E., Dufrêne, E., 2016. Wood phenology, not carbon input, controls the interannual variability of wood growth in a temperate oak forest. New Phytol. 210 (2), 459–470. https://doi.org/10.1111/nph.13771.
Díaz-Delgado, R., Lloret, F., Pons, X., Terradas, J., 2002. Satellite Evidence of Decreasing Resilience in Mediterranean Plant Communities After Recurrent Wildfires. Ecology 83, 2293–2303. https://doi.org/10.1890/0012-9658(2002)083[2293,SEODRI]2.0.CO, 2.
Díaz-Delgado, R., Lloret, F., Pons, X., 2004. Spatial patterns of fire occurrence in Catalonia, NE, Spain. Landsc. Ecol. 19, 731–745. https://doi.org/10.1007/s10980-005-0183-1.
Domingos, T., Kalapodis, N., Sakkas, G., Chandramouli, K., Gama, I., Proença, V., Ribeiro, I., Pio, M., 2025. Advancing Integrated Fire Management and Closer-to-Nature Forest Management: A Holistic Approach to Wildfire Risk Reduction and Ecosystem Resilience in Quinta da França. Portugal. *Forests* 16 (8), 1306. https://doi.org/10.3390/f16081306.
Druel, A., Ruffault, J., Davi, H., Chanzy, A., Marloie, O., De Cáceres, M., Olioso, A., Mouillot, F., François, C., Soudani, K., Martin-StPaul, N.K., 2025. Enhancing environmental models with a new downscaling method for global radiation in complex terrain. Biogeosciences 22 (1), 1–18. https://doi.org/10.5194/bg-22-1-2025.
Dubayah, R., Armston, J., Healey, S.P., Bruening, J.M., Patterson, P.L., Kellner, J.R., Duncanson, L., Saarela, S., Ståhl, G., Yang, Z., Tang, H., Blair, J.B., Fatoyinbo, L., Goetz, S., Hancock, S., Hansen, M., Hofton, M., Hurtt, G., Luthcke, S., 2022. GEDI launches a new era of biomass inference from space. Environ. Res. Lett. 17, 095001. https://doi.org/10.1088/1748-9326/ac8694.
Dupire, S., Bourrier, F., Monnet, J.-M., Berger, F., 2015. Sylvaccess: Un modèle pour cartographier automatiquement l'accessibilité des forêts. *Revue Forestière Française*, (2), Fr. ISSN 0035. https://doi.org/10.4267/2042/57902.
Dupire, S., Curt, T., Bigot, S., Fréjaville, T., 2019. Vulnerability of forest ecosystems to fire in the French Alps. Eur. J. For. Res. 138 (5), 813–830. https://doi.org/10.1007/s10342-019-01206-1.
Dyderski, M.K., Paź, S., Frelich, L.E., Jagodziński, A.M., 2018. How much does climate change threaten European forest tree species distributions? Glob. Chang. Biol. 24 (3), 1150–1163. https://doi.org/10.1111/gcb.13925.

El Garroussi, S., Di Giuseppe, F., Barnard, C., Wetterhall, F., 2024. Europe faces up to tenfold increase in extreme fires in a warming climate. npj Climate and Atmospheric Science 7, 30. https://doi.org/10.1038/s41612-024-00575-8.
Elvira, N.J., Lloret, F., Serra-Díaz, J.M., Sánchez Mejía, M.T., Codina Martínez, G., Batllori, E., 2026. Post-fire recovery is modulated by the position in the realized climatic niche in three Mediterranean tree species. For. Ecol. Manag. 600, 123301. https://doi.org/10.1016/j.foreco.2025.123301.
Epstein, M.D., Seielstad, C.A., Moran, C.J., 2024. Impact and recovery of forest cover following wildfire in the Northern Rocky Mountains of the United States. Fire Ecol. 20 (1), 56. https://doi.org/10.1186/s42408-024-00285-9.
Ermitao, T., Gouveia, C.M., Bastos, A., Russo, A.C., 2024. Recovery Following Recurrent Fires Across Mediterranean Ecosystems. Glob. Chang. Biol. 30 (12), e70013. https://doi.org/10.1111/gcb.70013.
Fernandes, P.M., 2015. Empirical Support for the Use of Prescribed Burning as a Fuel Treatment. Curr. For. Rep. 1, 118–127. https://doi.org/10.1007/s40725-015-0010-z.
Fernandes, P.M., Davies, G.M., Ascoli, D., Fernández, C., Moreira, F., Rigolot, E., Stoof, C. R., Vega, J.A., Molina, D., 2013. Prescribed burning in southern Europe: developing fire management in a dynamic landscape. Front. Ecol. Environ. 11. https://doi.org/10.1890/120298.
Fernández-Guisuraga, J.M., Calvo, L., Fernandes, P.M., Suárez-Seoane, S., 2022. Short-Term Recovery of the Aboveground Carbon Stock in Iberian Shrublands at the Extremes of an Environmental Gradient and as a Function of Burn Severity. Forests 13 (2), 145. https://doi.org/10.3390/f13020145.
Fernandez-Guisuraga, J.M., Fernandes, P.M., 2024. Prescribed burning mitigates the severity of subsequent wildfires in Mediterranean shrublands. Fire Ecol 20, 4. https://doi.org/10.1186/s42408-023-0233-z.
Finney, M.A., 2005. The challenge of quantitative risk analysis for wildland fire. Elsevier BV 211, 97–108. https://doi.org/10.1016/j.foreco.2005.02.010.
Forzieri, G., Girardello, M., Ceccherini, G., Spinoni, J., Feyen, L., Hartmann, H., Beck, P. S.A., Camps-Valls, G., Chirici, G., Mauri, A., Cescatti, A., 2021. Emergent vulnerability to climate-driven disturbances in European forests. Nat. Commun. 12 (1), 1081. https://doi.org/10.1038/s41467-021-21399-7.
Franquesa, M., Vanderhoof, M.K., Stavrakoudis, D., Gitas, I.Z., Roteta, E., Padilla, M., Chuvieco, E., 2020. Development of a standard database of reference sites for validating global burned area products. Earth System Science Data 12, 3229–3246. https://doi.org/10.5194/essd-12-3229-2020.
Galizia, L.F., Barbero, R., Rodrigues, M., Ruffault, J., Pimont, F., Curt, T., 2023. Global Warming Reshapes European Pyroregions. *Earth's*. Future 11 (5). https://doi.org/10.1029/2022EF003182 e2022EF003182.
García, M.J.L., Caselles, V., 1991. Mapping burns and natural reforestation using thematic Mapper data. Geocarto International 6, 31–37. https://doi.org/10.1080/10106049109354290.
GCOS | WMO. (2024). https://gcos.wmo.int/en/essential-climate-variables/fire. Last access : 16th July 2024, 2026.
Gonzalez-Akre, E., Piponiot, C., Lepore, M., Herrmann, V., Lutz, J.A., Baltzer, J.L., Dick, C.W., Gilbert, G.S., He, F., Heym, M., Huerta, A.I., Jansen, P.A., Johnson, D.J., Knapp, N., Král, K., Lin, D., Malhi, Y., McMahon, S.M., Myers, J.A., Orwig, D., Rodríguez-Hernández, D.I., Russo, S.E., Shue, J., Wang, X., Wolf, A., Yang, T., Davies, S.J., Anderson-Teixeira, K.J., 2022. allodb: An R package for biomass estimation at globally distributed extratropical forest plots. Methods Ecol. Evol. 13, 330–338. https://doi.org/10.1111/2041-210X.13756.
Guerra-Hernández, J., Pereira, J.M.C., Stovall, A., Pascual, A., 2024. Impact of fire severity on forest structure and biomass stocks using NASA GEDI data. Insights from the 2020 and 2021 wildfire season in Spain and Portugal. Science of Remote Sensing 9, 100134. https://doi.org/10.1016/j.srs.2024.100134.
Hagmann, R.K., Hessburg, P.F., Salter, R.B., Merschel, A.G., Reilly, M.J., 2022. Contemporary wildfires further degrade resistance and resilience of fire-excluded forests. For. Ecol. Manag. 506, 119975. https://doi.org/10.1016/j.foreco.2021.119975.
Hansen, M.C., Potapov, P.V., Moore, R., Hancher, M., Turubanova, S.A., Tyukavina, A., Thau, D., Stehman, S.V., Goetz, S.J., Loveland, T.R., Kommareddy, A., Egorov, A., Chini, L., Justice, C.O., Townshend, J.R.G., 2013. High-Resolution Global Maps of 21st-Century Forest Cover Change. Science 342 (6160), 850–853. https://doi.org/10.1126/science.1244693.
Harvey, B.J., Donato, D.C., Turner, M.G., 2016. High and dry: post-fire tree seedling establishment in subalpine forests decreases with post-fire drought and large stand-replacing burn patches. Glob. Ecol. Biogeogr. 25, 655–669. https://doi.org/10.1111/geb.12443.
Hawbaker, T.J., Vanderhoof, M.K., Schmidt, G.L., Beal, Y.-J., Picotte, J.J., Takacs, J.D., Falgout, J.T., Dwyer, J.L., 2020. The Landsat Burned Area algorithm and products for the conterminous United States. Remote Sens. Environ. 244, 111801. https://doi.org/10.1016/j.rse.2020.111801.
He, T., Pausas, J.G., Belcher, C.M., Schwilk, D.W., Lamont, B.B., 2012. Fire-adapted traits of Pinus arose in the fiery Cretaceous. The New Phytologist 194, 751–759. https://doi.org/10.1111/j.1469-8137.2012.04079.x.
Hengeveld, G.M., Nabuurs, G.-J., Didion, M., van den Wyngaert, I., Clerkx, A.P.P.M. Sandra, Schelhaas, M.-J., 2012. A Forest Management Map of European Forests. Ecol. Soc. 17 (4). https://doi.org/10.5751/ES-05149-17045.
Hérault, B., Piponiot, C., 2018. Key drivers of ecosystem recovery after disturbance in a neotropical forest: Long-term lessons from the Paracou experiment. French Guiana. *Forest Ecosystems* 5 (1), 2. https://doi.org/10.1186/s40663-017-0126-7.
Hersbach, H., Bell, B., Berrisford, P., Hirahara, S., Horányi, A., Muñoz-Sabater, J., Nicolas, J., Peubey, C., Radu, R., Schepers, D., Simmons, A., Soci, C., Abdalla, S., Abellan, X., Balsamo, G., Bechtold, P., Biavati, G., Bidlot, J., Bonavita, M., De Chiara, G., Dahlgren, P., Dee, D., Diamantakis, M., Dragani, R., Flemming, J., Forbes, R., Fuentes, M., Geer, A., Haimberger, L., Healy, S., Hogan, R.J., Hólm, E., Janisková, M., Keeley, S., Laloyaux, P., Lopez, P., Lupu, C., Radnoti, G., De Rosnay, P., Rozum, I., Vamborg, F., Villaume, S., Thépaut, J., 2020. The ERA5 global reanalysis. Q. J. R. Meteorol. Soc. 146, 1999–2049. https://doi.org/10.1002/qj.3803.
Hertzog, L.R., Piedallu, C., Lebourgeois, F., Bouriaud, O., Bontemps, J.-D., 2025. Turning point in the productivity of western European forests associated with a climate change footprint. Sci. Total Environ. 967, 178843. https://doi.org/10.1016/j.scitotenv.2025.178843.
Hijmans, R., 2025. terra: Spatial Data Analysis. R package version 1, 8–86. https://github.com/rspatial/terra.
Holik, J., Janik, D., Samonil, P., Hort, L., Kral, K., 2025. Topographic conditions dominate tree species recovery over 15 years post-fire in a temperate Pinus sylvestris forest. Fire Ecol. 21 (1), 29. https://doi.org/10.1186/s42408-025-00374-3.
Hu, T., Yu, C., Dou, X., Zhang, Y., Li, G., Sun, L., 2023. Simulation of Soil Organic Carbon Dynamics in Postfire Boreal Forests of China by Incorporating High-Resolution Remote Sensing Data and Field Measurement. Fire 6, 414. https://doi.org/10.3390/fire6110414.
Hunter, M.E., Robles, M.D., 2020. Tamm review: The effects of prescribed fire on wildfire regimes and impacts: A framework for comparison. For. Ecol. Manag. 475, 118435. https://doi.org/10.1016/j.foreco.2020.118435.
IGN: BD FORET. https://geoservices.ign.fr/bdforet, 2018.
Ingrisch, J., Bahn, M., 2018. Towards a Comparable Quantification of Resilience. Trends Ecol. Evol. 33 (4), 251–259. https://doi.org/10.1016/j.tree.2018.01.013.
Ireland, G., Petropoulos, G.P., 2015. Exploring the relationships between post-fire vegetation regeneration dynamics, topography and burn severity: A case study from the Montane Cordillera Ecozones of Western Canada. J. Appl. Geogr. 56, 232–248.
Jevšenak, J., Klisz, M., Mašek, J., Čada, V., Janda, P., Svoboda, M., Vostarek, O., Treml, V., Van Der Maaten, E., Popa, A., Popa, I., Van Der Maaten-Theunissen, M., Zlatanov, T., Scharnweber, T., Ahlgrimm, S., Stolz, J., Sochová, I., Roibu, C.-C., Pretzsch, H., Buras, A., 2024. Incorporating high-resolution climate, remote sensing and topographic data to map annual forest growth in central and eastern Europe. Sci. Total Environ. 913, 169692. https://doi.org/10.1016/j.scitotenv.2023.169692.
Johnstone, J.F., McIntire, E.J.B., Pedersen, E.J., King, G., Pisaric, M.J., 2010. F.: A sensitive slope: estimating landscape patterns of forest resilience in a changing climate. Ecosphere 1. https://doi.org/10.1890/ES10-00102.1 art14.
Jones, M.W., Abatzoglou, J.T., Veraverbeke, S., Andela, N., Lasslop, G., Forkel, M., Smith, A.J.P., Burton, C., Betts, R.A., van der Werf, G.R., Sitch, S., Canadell, J.G., Santín, C., Kolden, C., Doerr, S.H., Le Quéré, C., 2022. Global and Regional Trends and Drivers of Fire Under Climate Change. Rev. Geophys. 60. https://doi.org/10.1029/2020RG000726.
Jouy, F., Schüle, M., Adhikari, Y., Binder, A., Clerc, D., Gerwin, W., Heinken, T., Raab, T., Repmann, F., Rönnefarth, S., Schirrmacher, M., Schmehl, M., Schröder, J., Ibisch, P. L., 2025. Factors impacting the variability of post-fire forest regeneration in central European pine plantations. Restor. Ecol. 33 (4), e70017. https://doi.org/10.1111/rec.70017.
Jung, C.G., Keyser, A.R., Remy, C.C., Krofcheck, D., Allen, C.D., Hurteau, M.D., 2023. Topographic information improves simulated patterns of post-fire conifer regeneration in the southwest United States. Glob. Chang. Biol. 29 (15), 4342–4353. https://doi.org/10.1111/gcb.16764.
Kaiser, J.W., Heil, A., Andreae, M.O., Benedetti, A., Chubarova, N., Jones, L., Morcrette, J.-J., Razinger, M., Schultz, M.G., Suttie, M., Van Der Werf, G.R., 2012. Biomass burning emissions estimated with a global fire assimilation system based on observed fire radiative power. Biogeosciences 9, 527–554. https://doi.org/10.5194/bg-9-527-2012.
Kashian, D.M., Romme, W.H., Tinker, D.B., Turner, M.G., Ryan, M.G., 2013. Postfire changes in forest carbon storage over a 300-year chronosequence of *Pinus contorta* -dominated forests. Ecol. Monogr. 83 (1), 49–66. https://doi.org/10.1890/11-1454.1.
Kavanagh, K.L., Dickinson, M.B., Bova, A.S., 2010. A Way Forward for Fire-Caused Tree Mortality Prediction: Modeling A Physiological Consequence of Fire. Fire Ecol. 6 (1), 80–94. https://doi.org/10.4996/fireecology.0601080.
Kebrle, D., Zasadil, P., Hošek, J., Barták, V., Šťastný, K., 2021. Large trees as a key factor for bird diversity in spruce-dominated production forests: Implications for conservation management. For. Ecol. Manag. 496, 119460. https://doi.org/10.1016/j.foreco.2021.119460.
Kemp, K.B., Higuera, P.E., Morgan, P., Abatzoglou, J.T., 2019. Climate will increasingly determine post-fire tree regeneration success in low-elevation forests, Northern Rockies, USA. Ecosphere 10 (1), e02568. https://doi.org/10.1002/ecs2.2568.
Key, C.H., Benson, N.C., 1999. The normalized burn ratio (NBR): A landsat TM radiometric measure of burn severity. U. S. Geol. Surv. North. Rocky Mt. Sci. Cent, Bozeman MT USA.
Komlós, M., Botta-Dukát, Z., Bölöni, J., Aszalós, R., Veres, K., Winkler, D., Ónodi, G., 2024. Tall, large-diameter trees and dense shrub layer as key determinants of the abundance and composition of bird communities in oak-dominated forests. J. For. Res. 35, 62. https://doi.org/10.1007/s11676-024-01714-w.
Kouachi, M.E., Khairoun, A., Moghli, A., Rahmani, S., Mouillot, F., Baeza, M.J., Moutahir, H., 2024. Forty-Year Fire History Reconstruction from Landsat Data in Mediterranean Ecosystems of Algeria following International Standards. Remote Sens. 16, 2500. https://doi.org/10.3390/rs16132500.
Koutsias, N., Panourgia, K., Nakas, G., Petanidou, T., 2024. The importance of landscape and fire-history as factors explaining post-fire vegetation recovery in a Mediterranean island using Sentinel-2 satellite data. Sci. Total Environ. 957, 177443. https://doi.org/10.1016/j.scitotenv.2024.177443.
Kreuter, U.P., Wonkka, C.L., Twidwell, D., Treadwell, M.L., May, N.L., 2025. Awareness and Social Interactions Influence Natural Resource Professionals' Recommendations

for Prescribed Fire Use. Rangel. Ecol. Manag. 100, 89–98. https://doi.org/10.1016/j.rama.2025.02.003.
Kühn, I., Durka, W., Klotz, S., 2004. BiolFlor — a new plant-trait database as a tool for plant invasion ecology. Divers. Distrib. 10, 363–365. https://doi.org/10.1111/j.1366-9516.2004.00106.x.
Lamont, B.B., Pausas, J.G., He, T., Witkowski, E.T.F., Hanley, M.E., 2020. Fire as a Selective Agent for both Serotiny and Nonserotiny Over Space and Time. Crit. Rev. Plant Sci. 39 (2), 140–172. https://doi.org/10.1080/07352689.2020.1768465.
Lecina-Diaz, J., Martínez-Vilalta, J., Alvarez, A., Banqué, M., Birkmann, J., Feldmeyer, D., Vayreda, J., Retana, J., 2021. Characterizing forest vulnerability and risk to climate-change hazards. Front. Ecol. Environ. 19 (2), 126–133. https://doi.org/10.1002/fee.2278.
Lempereur, M., Limousin, J., Guibal, F., Ourcival, J., Rambal, S., Ruffault, J., Mouillot, F., 2017. Recent climate hiatus revealed dual control by temperature and drought on the stem growth of Mediterranean *Quercus ilex*. Glob. Chang. Biol. 23 (1), 42–55. https://doi.org/10.1111/gcb.13495.
Li, Y., Li, Q., Xu, L., Li, M., Chen, Z., Song, Z., Hou, J., He, N., 2021. Plant community traits can explain variation in productivity of selective logging forests after different restoration times. Ecol. Indic. 131, 108181. https://doi.org/10.1016/j.ecolind.2021.108181.
Liang, M., González-Roglich, M., Roehrdanz, P., Tabor, K., Zvoleff, A., Leitold, V., Silva, J., Fatoyinbo, T., Hansen, M., Duncanson, L., 2023. Assessing protected area's carbon stocks and ecological structure at regional-scale using GEDI lidar. Glob. Environ. Chang. 78, 102621. https://doi.org/10.1016/j.gloenvcha.2022.102621.
Lippok, D., Beck, S.G., Renison, D., Gallegos, S.C., Saavedra, F.V., Hensen, I., Schleuning, M., 2013. Forest recovery of areas deforested by fire increases with elevation in the tropical Andes. For. Ecol. Manag. 295, 69–76. https://doi.org/10.1016/j.foreco.2013.01.011.
Liu, Q., Fu, B., Chen, Z., Chen, L., Liu, L., Peng, W., Liang, Y., Chen, L., 2022. Evaluating Effects of Post-Fire Climate and Burn Severity on the Early-Term Regeneration of Forest and Shrub Communities in the San Gabriel Mountains of California from Sentinel-2(MSI) Images. Forests 13, 1060. https://doi.org/10.3390/f13071060.
LOI N° 2023-580 Du 10 Juillet 2023 Visant à Renforcer La Prévention et La Lutte Contre l'intensification et l'extension Du Risque Incendie (1), 2023-580. https://www.legifrance.gouv.fr/jorf/id/JORFTEXT000047805414.
Lojo, A., Musić, J., Balić, B., Avdagić, A., Halilović, V., Ibrahimspahić, A., Knežević, J., 2021. Modeling bark thickness of beech (*Fagus sylvatica* L.). Šumar. List 145, 239–247. https://doi.org/10.31298/sl.145.5-6.3.
Lososova, Z., Axmanová, I., Chytrý, M., Midolo, G., Abdulhak, S., Karger, D.N., Renaud, J., Van Es, J., Vittoz, P., Thuiller, W., 2023. Seed dispersal distance classes and dispersal modes for the European flora. Glob. Ecol. Biogeogr. 32 (9), 1485–1494. https://doi.org/10.1111/geb.13712.
Lucas-Borja, M.E., Delgado-Baquerizo, M., Muñoz-Rojas, M., Plaza-Álvarez, P.A., Gómez-Sanchez, M.E., González-Romero, J., Peña-Molina, E., Moya, D., De Las Heras, J., 2021. Changes in ecosystem properties after post-fire management strategies in wildfire-affected Mediterranean forests. J. Appl. Ecol. 58 (4), 836–846. https://doi.org/10.1111/1365-2664.13819.
Lv, Q., Chen, Z., Wu, C., Peñuelas, J., Fan, L., Su, Y., Yang, Z., Li, M., Gao, B., Hu, J., Zhang, C., Fu, Y., Wang, Q., 2025. Increasing severity of large-scale fires prolongs recovery time of forests globally since 2001. Nature Ecology & Evolution 9 (6), 980–992. https://doi.org/10.1038/s41559-025-02683-x.
Majdalani, G., Koutsias, N., Faour, G., Adjizian-Gerard, J., Mouillot, F., 2022. Fire Regime Analysis in Lebanon (2001–2020): Combining Remote Sensing Data in a Scarcely Documented Area. Fire 5, 141. https://doi.org/10.3390/fire5050141.
Manela, N., Shemesh, H., Osem, Y., Carmel, Y., Soref, C., Tsafrir, A., Ovadia, O., 2022. Seasonal fires shape the germinable soil seed bank community in eastern Mediterranean woodlands. J. Plant Ecol. 15 (1), 13–25. https://doi.org/10.1093/jpe/rtab070.
Maringer, J., Ascoli, D., Küffer, N., Schmidtlein, S., Conedera, M., 2016. What drives European beech (Fagus sylvatica L.) mortality after forest fires of varying severity? For. Ecol. Manag. 368, 81–93. https://doi.org/10.1016/j.foreco.2016.03.008.
Martinez Del Castillo, E., Zang, C.S., Buras, A., Hacket-Pain, A., Esper, J., Serrano-Notivoli, R., Hartl, C., Weigel, R., Klesse, S., Resco De Dios, V., Scharnweber, T., Dorado-Liñán, I., Van Der Maaten-Theunissen, M., Van Der Maaten, E., Jump, A., Mikac, S., Banzragch, B.-E., Beck, W., Cavin, L., De Luis, M., 2022. Climate-change-driven growth decline of European beech forests. Communications Biology 5 (1), 163. https://doi.org/10.1038/s42003-022-03107-3.
Mauri, A., Girardello, M., Strona, G., Beck, P.S.A., Forzieri, G., Caudullo, G., Manca, F., Cescatti, A., 2022. EU-Trees4F, a dataset on the future distribution of European tree species. Sci. Data 9, 37. https://doi.org/10.1038/s41597-022-01128-5.
Meier, S., Elliott, R.J.R., Strobl, E., 2023. The regional economic impact of wildfires: Evidence from Southern Europe. J. Environ. Econ. Manag. 118, 102787. https://doi.org/10.1016/j.jeem.2023.102787.
Meng, R., Dennison, P.E., Huang, C., Moritz, M.A., D'Antonio, C., 2015. Effects of fire severity and post-fire climate on short-term vegetation recovery of mixed-conifer and red fir forests in the Sierra Nevada Mountains of California. Remote Sens. Environ. 171, 311–325. https://doi.org/10.1016/j.rse.2015.10.024.
Miettinen, J., Breidenbach, J., Adame, P., Adolt, R., Alberdi, I., Antropov, O., Arnarsson, Ó., Astrup, R., Berger, A., Bogason, J., Chirici, G., Corona, P., D'Amico, G., Fejfar, J., Fischer, C., Gohon, F., Gschwantner, T., Hertzler, J., Koma, Z., Wurpillot, S., 2025. Pan-European forest maps produced with a combination of earth observation data and national forest inventory plots. Data in Brief 60, 111613. https://doi.org/10.1016/j.dib.2025.111613.
Miller, R.G., Fontaine, J.B., Merritt, D.J., Miller, B.P., Enright, N.J., 2021. Experimental seed sowing reveals seedling recruitment vulnerability to unseasonal fire. Ecol. Appl. 31 (7), e02411. https://doi.org/10.1002/eap.2411.
Moreira, F., Arianoutsou, M., Corona, P., 2012. & De Las Heras. In: J. (Ed.), Post-Fire Management and Restoration of Southern European Forests, 24. Springer, Netherlands. https://doi.org/10.1007/978-94-007-2208-8.
Morin, X., Bugmann, H., de Coligny, F., Martin-StPaul, N., Cailleret, M., Limousin, J., Ourcival, J., Prévosto, B., Simioni, G., Toïgo, M., Vennetier, M., Catteau, E., Guillemot, J., 2021. Beyond forest succession: A gap model to study ecosystem functioning and tree community composition under climate change. Wiley-Blackwell 35, 955–975. https://doi.org/10.1111/1365-2435.13760.
Moris, J.V., Reilly, M.J., Yang, Z., Cohen, W.B., Motta, R., Ascoli, D., 2022. Using a trait-based approach to asses fire resistance in forest landscapes of the Inland Northwest, USA. Landsc. Ecol. 37 (8), 2149–2164. https://doi.org/10.1007/s10980-022-01478-w.
Mouillot, F., Rambal, S., Lavorel, S., 2001. A generic process-based simulator for Mediterranean Landscapes (SIERRA): design and validation exercises. For. Ecol. Manag. 147 (1), 75–97.https. https://doi.org/10.1016/S0378-1127(00)00432-1.
Mouillot, F., Ratte, J.-P., Joffre, R., Mouillot, D., Serge Rambal, A., 2005. Long-term forest dynamic after land abandonment in a fire prone Mediterranean landscape (central Corsica, France). Landsc. Ecol. 20 (1), 101–112. https://doi.org/10.1007/s10980-004-1297-5.
Mouillot, D., Velez, L., Albouy, C., Casajus, N., Claudet, J., Delbar, V., Devillers, R., Letessier, T.B., Loiseau, N., Manel, S., Mannocci, L., Meeuwig, J., Mouquet, N., Nuno, A., O'Connor, L., Parravicini, V., Renaud, J., Seguin, R., Troussellier, M., Thuiller, W., 2024. The socioeconomic and environmental niche of protected areas reveals global conservation gaps and opportunities. Nat. Commun. 15 (1), 9007. https://doi.org/10.1038/s41467-024-53241-1.
Neidermeier, A.N., Zagaria, C., Pampanoni, V., West, T.A.P., Verburg, P.H., 2023. Mapping opportunities for the use of land management strategies to address fire risk in Europe. J. Environ. Manag. 346, 118941. https://doi.org/10.1016/j.jenvman.2023.118941.
Nelson, Z.J., Weisberg, P.J., Kitchen, S.G., 2014. Influence of climate and environment on post-fire recovery of mountain big sagebrush. Int. J. Wildland Fire 23, 131. https://doi.org/10.1071/WF13012.
Noble, I.R., Slatyer, R.O., 1980. The use of vital attributes to predict successional changes in plant communities subject to recurrent disturbances. Vegetatio 43, 5–21. https://doi.org/10.1007/BF00121013.
Noon, M.L., Goldstein, A., Ledezma, J.C., Roehrdanz, P.R., Cook-Patton, S.C., Spawn-Lee, S.A., Wright, T.M., Gonzalez-Roglich, M., Hole, D.G., Rockström, J., Turner, W. R., 2021. Mapping the irrecoverable carbon in Earth's ecosystems. Nat. Sustainability 5 (1), 37–46. https://doi.org/10.1038/s41893-021-00803-6.
Oliveira, S., Félix, F., Nunes, A., Lourenço, L., Laneve, G., Sebastián-López, A., 2018. Mapping wildfire vulnerability in Mediterranean Europe. Testing a stepwise approach for operational purposes. J. Environ. Manag. 206, 158–169. https://doi.org/10.1016/j.jenvman.2017.10.003.
Oliveira, S., Gonçalves, A., Benali, A., Sá, A., Zêzere, J.L., Pereira, J.M., 2020. Assessing Risk and Prioritizing Safety Interventions in Human Settlements Affected by Large Wildfires. Forests 11 (8). https://doi.org/10.3390/f11080859. Article 8.
Oliveras Menor, I., Prat-Guitart, N., Spadoni, G.L., Hsu, A., Fernandes, P.M., Puig-Gironès, R., Ascoli, D., Bilbao, B.A., Bacciu, V., Brotons, L., Carmenta, R., de Miguel, S., Gonçalves, L.G., Humphrey, G., Ibarnegaray, V., Jones, M.W., Machado, M.S., Millán, A., de Morais Falleiro, R., Armenteras Pascual, D., 2025. Integrated fire management as an adaptation and mitigation strategy to altered fire regimes. Commun. Earth Environ. 6 (1), 202. https://doi.org/10.1038/s43247-025-02165-9.
Ouattara, B., Thiel, M., Forkuor, G., Mouillot, F., Laris, P., Tondoh, E.J., Sponholz, B., 2025. Fire Impacts, vegetation Recovery, and environmental drivers in West African savannas (2014–2023): A High-Resolution remote sensing assessment. Int. J. Appl. Earth Obs. Geoinf. 143, 104783. https://doi.org/10.1016/j.jag.2025.104783.
Pacheco, R.M., Claro, J., 2021. Prescribed burning as a cost-effective way to address climate change and forest management in Mediterranean countries. Ann. For. Sci. 78, 100. https://doi.org/10.1007/s13595-021-01115-7.
Palviainen, M., Laurén, A., Pumpanen, J., Bergeron, Y., Bond-Lamberty, B., Larjavaara, M., Kashian, D.M., Köster, K., Prokushkin, A., Chen, H.Y.H., Seedre, M., Wardle, D.A., Gundale, M.J., Nilsson, M.-C., Wang, C., Berninger, F., 2020. Decadal-Scale Recovery of Carbon Stocks After Wildfires Throughout the Boreal Forests. Glob. Biogeochem. Cycles 34 (8). https://doi.org/10.1029/2020GB006612 e2020GB006612.
Parks, S., Holsinger, L., Voss, M., Loehman, R., Robinson, N., 2018. Mean Composite Fire Severity Metrics Computed with Google Earth Engine Offer Improved Accuracy and Expanded Mapping Potential. Remote Sens. 10, 879. https://doi.org/10.3390/rs10060879.
Parra, A., Moreno, J.M., 2018. Drought differentially affects the post-fire dynamics of seeders and resprouters in a Mediterranean shrubland. Sci. Total Environ. 626, 1219–1229. https://doi.org/10.1016/j.scitotenv.2018.01.174.
Patacca, M., Lindner, M., Lucas-Borja, M.E., Cordonnier, T., Fidej, G., Gardiner, B., Hauf, Y., Jasinevičius, G., Labonne, S., Linkevičius, E., Mahnken, M., Milanovic, S., Nabuurs, G., Nagel, T.A., Nikinmaa, L., Panyatov, M., Bercak, R., Seidl, R., Ostrogović Sever, M.Z., Schelhaas, M., 2023. Significant increase in natural disturbance impacts on European forests since 1950. Glob. Chang. Biol. 29 (5), 1359–1376. https://doi.org/10.1111/gcb.16531.
Pausas, J.G., 2004. Changes in Fire and Climate in the Eastern Iberian Peninsula (Mediterranean Basin). Clim. Chang. 63, 337–350. https://doi.org/10.1023/B:CLIM.0000018508.94901.9c.
Pausas, J.G., 2015. Bark thickness and fire regime. Funct. Ecol. 29 (3), 315–327. https://doi.org/10.1111/1365-2435.12372.
Pausas, J.G., Pratt, R.B., Keeley, J.E., Jacobsen, A.L., Ramirez, A.R., Vilagrosa, A., Paula, S., Kaneakua-Pia, I.N., Davis, S.D., 2016. Towards understanding resprouting

at the global scale. The New Phytologist 209, 945–954. https://doi.org/10.1111/nph.13644.
Pausas, J.G., Lamont, B.B., Paula, S., Appezzato-da-Glória, B., Fidélis, A., 2018. Unearthing belowground bud banks in fire-prone ecosystems. Wiley-Blackwell 217 (4), 1435–1448. https://doi.org/10.1111/nph.14982.
Pellegrini, A.F.A., Anderegg, W.R.L., Paine, C.E.T., Hoffmann, W.A., Kartzinel, T., Rabin, S.S., Sheil, D., Franco, A.C., Pacala, S.W., 2017. Convergence of bark investment according to fire and climate structures ecosystem vulnerability to future change. Ecol. Lett. 20, 307–316. https://doi.org/10.1111/ele.12725.
Pellissier-Tanon, A., Ciais, P., Schwartz, M., Fayad, I., Xu, Y., Ritter, F., De Truchis, A., Leban, J.-M., 2024. Combining satellite images with national forest inventory measurements for monitoring post-disturbance forest height growth. Frontiers in Remote Sensing 5, 1432577. https://doi.org/10.3389/frsen.2024.1432577.
Pereira, H.M., Ferrier, S., Walters, M., Geller, G.N., Jongman, R.H.G., Scholes, R.J., Bruford, M.W., Brummitt, N., Butchart, S.H.M., Cardoso, A.C., Coops, N.C., Dulloo, E., Faith, D.P., Freyhof, J., Gregory, R.D., Heip, C., Höft, R., Hurtt, G., Jetz, W., Wegmann, M., 2013. Essential Biodiversity Variables. Science 339 (6117), 277–278. https://doi.org/10.1126/science.1229931.
Perret, D.L., Evans, M.E.K., Sax, D.F., 2024. A species' response to spatial climatic variation does not predict its response to climate change. Proc. Natl. Acad. Sci. 121 (1), e2304404120. https://doi.org/10.1073/pnas.2304404120.
Pimont, F., Fargeon, H., Opitz, T., Ruffault, J., Barbero, R., Martin-StPaul, N., Rigolot, É., Rivière, M., Dupuy, J., 2021. Prediction of regional wildfire activity in the probabilistic Bayesian framework of Firelihood. Wiley-Blackwell 31. https://doi.org/10.1002/eap.2316.
Piñol, J., Beven, K., Viegas, D.X., 2005. Modelling the effect of fire-exclusion and prescribed fire on wildfire size in Mediterranean ecosystems. Ecol. Model. 183, 397–409. https://doi.org/10.1016/j.ecolmodel.2004.09.001.
Plana, E., Serra, M., Smeenk, A., Regos, A., Berchtold, C., Huertas, M., Fuentes, L., Trasobares, A., Vinders, J.N., Colaço, C., Bonet, J.A., 2024. Framing Coherence Across EU Policies Towards Integrated Wildfire Risk Management and Nature-Based Solutions. Fire 7, 415. https://doi.org/10.3390/fire7110415.
Potapov, P., Li, X., Hernandez-Serna, A., Tyukavina, A., Hansen, M.C., Kommareddy, A., Pickens, A., Turubanova, S., Tang, H., Silva, C.E., Armston, J., Dubayah, R., Blair, J. B., Hofton, M., 2021. Mapping global forest canopy height through integration of GEDI and Landsat data. Remote Sens. Environ. 253, 112165. https://doi.org/10.1016/j.rse.2020.112165.
Pretzsch, H., Del Río, M., Arcangeli, C., Bielak, K., Dudzinska, M., Forrester, D.I., Klädtke, J., Kohnle, U., Ledermann, T., Matthews, R., Nagel, J., Nagel, R., Ningre, F., Nord-Larsen, T., Biber, P., 2023. Forest growth in Europe shows diverging large regional trends. Sci. Rep. 13 (1), 15373. https://doi.org/10.1038/s41598-023-41077-6.
Prodon, R., Diaz-Delgado, R., 2021. Assessing the postfire resilience of a Mediterranean forest from satellite and ground data (NDVI, vegetation profile, avifauna). Écoscience 28 (1), 81–91. https://doi.org/10.1080/11956860.2021.1871826.
Puntieri, J.G., 1993. The self-thinning rule: bibliography revision. Preslia 65, 243–267.
Putman, E.B., Popescu, S.C., Eriksson, M., Zhou, T., Klockow, P., Vogel, J., Moore, G.W., 2018. Detecting and quantifying standing dead tree structural loss with reconstructed tree models using voxelized terrestrial lidar data. Remote Sens. Environ. 209, 52–65. https://doi.org/10.1016/j.rse.2018.02.028.
Reich, P.B., Luo, Y., Bradford, J.B., Poorter, H., Perry, C.H., Oleksyn, J., 2014. Temperature drives global patterns in forest biomass distribution in leaves, stems, and roots. Proc. Natl. Acad. Sci. 111 (38), 13721–13726. https://doi.org/10.1073/pnas.1216053111.
Reilly, M.J., Zuspan, A., Yang, Z., 2023. Characterizing post-fire delayed tree mortality with remote sensing: Sizing up the elephant in the room. Fire Ecol. 19 (1), 64. https://doi.org/10.1186/s42408-023-00223-1.
Resco De Dios, V., Cunill Camprubí, À., Campos-Arceiz, A., Clarke, H., He, Y., Zveushe, O.K., Domènech, R., Ying, H., Yao, Y., 2025a. Protected Areas Show Substantial and Increasing Risk of Wildfire Globally. Fire 8 (10), 405. https://doi.org/10.3390/fire8100405.
Resco De Dios, V., Schütze, S.J., Cunill Camprubí, À., Balaguer-Romano, R., Boer, M.M., Fernandes, P.M., 2025b. Protected areas as hotspots of wildfire activity in fire-prone Temperate and Mediterranean biomes. J. Environ. Manag. 385, 125669. https://doi.org/10.1016/j.jenvman.2025.125669.
Restor. https://restor.eco/, 2024 last access: 16 July 2024.
Rezgui, F., Mouillot, F., Semmar, N., Zribi, L., Khaldi, A., Nasr, Z., Gharbi, F., 2024. Assessment of Pinus halepensis Forests' Vulnerability Using the Temporal Dynamics of Carbon Stocks and Fire Traits in Tunisia. Fire 7, 204. https://doi.org/10.3390/fire7060204.
RGE ALTI® | Géoservices. https://geoservices.ign.fr/documentation/donnees/alti/rgealti, 2024 last access: 23 May 2024.
Rivière, M., Lenglet, J., Noirault, A., Pimont, F., Dupuy, J.-L., 2023. Mapping territorial vulnerability to wildfires: A participative multi-criteria analysis. For. Ecol. Manag. 539, 121014. https://doi.org/10.1016/j.foreco.2023.121014.
Rocha, M.R., Gaedke, U., Vasseur, D.A., 2011. Functionally similar species have similar dynamics. J. Ecol. 99 (6), 1453–1459. https://doi.org/10.1111/j.1365-2745.2011.01893.x.
Rodman, K.C., Veblen, T.T., Andrus, R.A., Enright, N.J., Fontaine, J.B., Gonzalez, A.D., Redmond, M.D., Wion, A.P., 2021. A trait-based approach to assessing resistance and resilience to wildfire in two iconic North American conifers. J. Ecol. 109 (1), 313–326. https://doi.org/10.1111/1365-2745.13480.
Rodrigues, M., Cunill Camprubí, À., Balaguer-Romano, R., Coco Megía, C.J., Castañares, F., Ruffault, J., Fernandes, P.M., Resco de Dios, V., 2023. Drivers and implications of the extreme 2022 wildfire season in Southwest Europe. Sci. Total Environ. 859 (160320). https://doi.org/10.1016/j.scitotenv.2022.160320.
Rodrigues, M., De La Riva, J., Domingo, D., Lamelas, T., Ibarra, P., Hoffrén, R., García-Martín, A., 2024. An empirical assessment of the potential of post-fire recovery of tree-forest communities in Mediterranean environments. For. Ecol. Manag. 552, 121587. https://doi.org/10.1016/j.foreco.2023.121587.
Roman Dobarco, M., Bourennane, H., Arrouays, D., Saby, N., Cousin, I., Martin, M.P., 2022. Réservoir utile des sols de la France métropolitaine. https://doi.org/10.15454/9IRARJ.
Rosell, J.A., 2016. Bark thickness across the angiosperms: more than just fire. The New Phytologist 211, 90–102. https://doi.org/10.1111/nph.13889.
Roteta, E., Bastarrika, A., Franquesa, M., Chuvieco, E., 2021. Landsat and Sentinel-2 Based Burned Area Mapping Tools in Google Earth Engine. Remote Sens. 13, 816. https://doi.org/10.3390/rs13040816.
Rouse, J.W., Haas, R.H., Deering, D.W., Schell, J.A., Harlan, J.C., 1974. Monitoring the Vernal Advancement and Retrogradation. (Green Wave Effect) of Natural Vegetation.
Ruffault, J., Martin-StPaul, N.K., Rambal, S., Mouillot, F., 2013. Differential regional responses in drought length, intensity and timing to recent climate changes in a Mediterranean forested ecosystem. Clim. Chang. 117 (1–2), 103–117. https://doi.org/10.1007/s10584-012-0559-5.
Ruffault, J., Martin-StPaul, N. K., Duffet, C., Goge, F., & Mouillot, F. (2014). Projecting future drought in Mediterranean forests: Bias correction of climate models matters! Theor. Appl. Climatol., 117(1–2), 113–122. doi:https://doi.org/10.1007/s00704-013-0992-z.
Ruffault, J., Curt, T., Moron, V., Trigo, R.M., Mouillot, F., Koutsias, N., Pimont, F., Martin-StPaul, N., Barbero, R., Dupuy, J.-L., Russo, A., Belhadj-Khedher, C., 2020. Increased likelihood of heat-induced large wildfires in the Mediterranean Basin. Sci. Rep. 10, 13790. https://doi.org/10.1038/s41598-020-70069-z.
Salesa, D., Baeza, M.J., Pérez-Ferrándiz, E., Santana, V.M., 2022. Longer summer seasons after fire induce permanent drought legacy effects on Mediterranean plant communities dominated by obligate seeders. Sci. Total Environ. 822, 153655. https://doi.org/10.1016/j.scitotenv.2022.153655.
Salis, M., Del Giudice, L., Alcasena-Urdiroz, F., Jahdi, R., Arca, B., Pellizzaro, G., Scarpa, C., Duce, P., 2023. Assessing cross-boundary wildfire hazard, transmission, and exposure to communities in the Italy-France Maritime cooperation area. Frontiers in Forests and Global Change 6. https://doi.org/10.3389/ffgc.2023.1241378.
Santoro, M., Cartus, O., Araza, A., Herold, M., Miettinen, J., Rosenqvist, A., Kobayashi, K., Tadono, T., Seifert, F.M., 2026. Europe-wide maps of biomass density based on satellite remote sensing data for 2017, 2020, 2021 and 2023. Data in Brief 65, 112536. https://doi.org/10.1016/j.dib.2026.112536.
Saulino, L., Rita, A., Stinca, A., Liuzzi, G., Silvestro, R., Rossi, S., Saracino, A., 2023. Wildfire promotes the invasion of Robinia pseudoacacia in the unmanaged Mediterranean Castanea sativa coppice forests. Frontiers in Forests and Global Change 6. https://doi.org/10.3389/ffgc.2023.1177551.
Schneider, F., Klinge, M., Brodthuhn, J., Peplau, T., Sauer, D., 2021. Hydrological soil properties control tree regrowth after forest disturbance in the forest steppe of central Mongolia. SOIL 7 (2), 563–584. https://doi.org/10.5194/soil-7-563-2021.
Schwartz, M., Ciais, P., De Truchis, A., Chave, J., Ottlé, C., Vega, C., Wigneron, J.-P., Nicolas, M., Jouaber, S., Liu, S., Brandt, M., Fayad, I., 2023. FORMS: Forest Multiple Source height, wood volume, and biomass maps in France at 10 to 30m resolution based on Sentinel-1, Sentinel-2, and Global Ecosystem Dynamics Investigation (GEDI) data with a deep learning approach. Earth Syst. Sci. Data 15, 4927–4945. https://doi.org/10.5194/essd-15-4927-2023.
Schwartz, M., Ciais, P., Sean, E., De Truchis, A., Vega, C., Besic, N., Fayad, I., Wigneron, J.-P., Brood, S., Pelissier-Tanon, A., Pauls, J., Belouze, G., Xu, Y., 2025. Retrieving yearly forest growth from satellite data: A deep learning based approach. Remote Sens. Environ. 330, 114959. https://doi.org/10.1016/j.rse.2025.114959.
Schwörer, C., Henne, P.D., Tinner, W., 2014. A model-data comparison of Holocene timberline changes in the Swiss Alps reveals past and future drivers of mountain forest dynamics. Glob. Chang. Biol. 20 (5), 1512–1526. https://doi.org/10.1111/gcb.12456.
Senande-Rivera, M., Insua-Costa, D., Miguez-Macho, G., 2022. Spatial and temporal expansion of global wildland fire activity in response to climate change. Nat. Commun. 13 (1), 1208. https://doi.org/10.1038/s41467-022-28835-2.
Senf, C., Seidl, R., 2020. Mapping the forest disturbance regimes of Europe. Nat. Sustainability 4 (1), 63–70. https://doi.org/10.1038/s41893-020-00609-y.
Sexton, J.O., Song, X.-P., Feng, M., Noojipady, P., Anand, A., Huang, C., Kim, D.-H., Collins, K.M., Channan, S., DiMiceli, C., Townshend, J.R., 2013. Global, 30-m resolution continuous fields of tree cover: Landsat-based rescaling of MODIS vegetation continuous fields with lidar-based estimates of error. International Journal of Digital Earth 6, 427–448. https://doi.org/10.1080/17538947.2013.786146.
Shen, Y., Prentice, I.C., Harrison, S.P., 2025. Investigation of factors that affect post-fire recovery of photosynthetic activity at global scale. Ecol. Indic. 171, 113206. https://doi.org/10.1016/j.ecolind.2025.113206.
Skakun, R., Castilla, G., Jain, P., 2024. Mapping wildfires in Canada with Landsat MSS to extend the National Burned Area Composite (NBAC) time series back to 1972. Int. J. Wildland Fire 33 (12), WF24138. https://doi.org/10.1071/WF24138.
Smithwick, E.A.H., Wu, H., Spangler, K., Adib, M., Wang, R., Dems, C., Taylor, A., Kaye, M., Zipp, K., Newman, P., Miller, Z.D., Zhao, A., 2024. Barriers and opportunities for implementing prescribed fire: Lessons from managers in the mid-Atlantic region. United States. Fire Ecology 20 (1), 77. https://doi.org/10.1186/s42408-024-00315-6.
Sørensen, R., Zinko, U., Seibert, J., 2006. On the calculation of the topographic wetness index: evaluation of different methods based on field observations. Hydrol. Earth Syst. Sci. Discuss. 10, 101–112.

Spatola, M.F., Borghetti, M., Nolè, A., 2023. Elucidating factors driving post-fire vegetation recovery in the Mediterranean forests using Landsat spectral metrics. Agric. For. Meteorol. 342, 109731. https://doi.org/10.1016/j.agrformet.2023.109731.

Stone, K.R., 2009. Robinia pseudoacacia. Fire Effects Information System.

Sweeney, K., Dittrich, R., Moffat, S., Power, C., Kline, J.D., 2023. Estimating the economic value of carbon losses from wildfires using publicly available data sources: Eagle Creek Fire, Oregon 2017. Fire Ecol. 19 (1), 55. https://doi.org/10.1186/s42408-023-00206-2.

Tangney, R., Merritt, D.J., Callow, J.N., Fontaine, J.B., Miller, B.P., 2020. Seed traits determine species' responses to fire under varying soil heating scenarios. Funct. Ecol. 34 (9), 1967–1978. https://doi.org/10.1111/1365-2435.13623.

Tangney, R., Paroissien, R., Le Breton, T.D., Thomsen, A., Doyle, C.A.T., Ondik, M., Miller, R.G., Miller, B.P., Ooi, M.K.J., 2022. Success of post-fire plant recovery strategies varies with shifting fire seasonality. Commun. Earth Environ. 3 (1), 126. https://doi.org/10.1038/s43247-022-00453-2.

Tavşanoğlu, Ç., Pausas, J.G., 2018. A functional trait database for Mediterranean Basin plants. Sci. Data 5 (1), 180135. https://doi.org/10.1038/sdata.2018.135.

Tepley, A.J., Thompson, J.R., Epstein, H.E., Anderson-Teixeira, K.J., 2017. Vulnerability to forest loss through altered postfire recovery dynamics in a warming climate in the Klamath Mountains. Glob. Chang. Biol. 23 (10), 4117–4132. https://doi.org/10.1111/gcb.13704.

Thornthwaite, C.W., 1948. An Approach toward a Rational Classification of Climate. Geogr. Rev. 38, 55. https://doi.org/10.2307/210739.

Trang, P.T., Andrew, M.E., Enright, N.J., 2023. Burn severity and proximity to undisturbed forest drive post-fire recovery in the tropical montane forests of northern Vietnam. Fire Ecol. 19 (1), 47. https://doi.org/10.1186/s42408-023-00205-3.

Trouve, R., Osborne, L., Baker, P.J., 2021. The effect fo species, size and fire intensity on tree mortality within a catastrophic bushfire complex. Ecol. Appl. 31 (6), e02383. https://doi.org/10.1002/eap.2383.

Trucchia, A., Meschi, G., Fiorucci, P., Provenzale, A., Tonini, M., Pernice, U., 2023. Wildfire hazard mapping in the eastern Mediterranean landscape. Int. J. Wildland Fire 32, 417–434. https://doi.org/10.1071/WF22138.

Turco, M., Von Hardenberg, J., AghaKouchak, A., Llasat, M.C., Provenzale, A., Trigo, R. M., 2017. On the key role of droughts in the dynamics of summer fires in Mediterranean Europe. Sci. Rep. 7 (1), 81. https://doi.org/10.1038/s41598-017-00116-9.

Turubanova, S., Potapov, P., Hansen, M.C., Li, X., Tyukavina, A., Pickens, A.H., Hernandez-Serna, A., Arranz, A.P., Guerra-Hernandez, J., Senf, C., Häme, T., Valbuena, R., Eklundh, L., Brovkina, O., Navrátilová, B., Novotný, J., Harris, N., Stolle, F., 2023. Tree canopy extent and height change in Europe, 2001–2021, quantified using Landsat data archive. Remote Sens. Environ. 298, 113797. https://doi.org/10.1016/j.rse.2023.113797.

Vallet, L., Schwartz, M., Ciais, P., Van Wees, D., De Truchis, A., Mouillot, F., 2023. High-resolution data reveal a surge of biomass loss from temperate and Atlantic pine forests, contextualizing the 2022 fire season distinctiveness in France. Biogeosciences 20, 3803–3825. https://doi.org/10.5194/bg-20-3803-2023.

Vallet, L., Abdallah, C., Lauvaux, T., Joly, L., Ramonet, M., Ciais, P., Lopez, M., Xueref-Remy, I., Mouillot, F., 2025. Soil smoldering in temperate forests: A neglected contributor to fire carbon emissions revealed by atmospheric mixing ratios. Biogeosciences 22 (1), 213–242. https://doi.org/10.5194/bg-22-213-2025.

Van Wees, D., Van Der Werf, G.R., Randerson, J.T., Rogers, B.M., Chen, Y., Veraverbeke, S., Giglio, L., Morton, D.C., 2022. Global biomass burning fuel consumption and emissions at 500 m spatial resolution based on the Global Fire Emissions Database (GFED). Geosci. Model Dev. 15, 8411–8437. https://doi.org/10.5194/gmd-15-8411-2022.

Viana-Soto, A., Aguado, I., Salas, J., García, M., 2020. Identifying Post-Fire Recovery Trajectories and Driving Factors Using Landsat Time Series in Fire-Prone Mediterranean Pine Forests. Remote Sens. 12 (9), 1499. https://doi.org/10.3390/rs12091499.

Viana-Soto, A., García, M., Aguado, I., Salas, J., 2022. Assessing post-fire forest structure recovery by combining LiDAR data and Landsat time series in Mediterranean pine forests. Int. J. Appl. Earth Obs. Geoinf. 108, 102754. https://doi.org/10.1016/j.jag.2022.102754.

Vicente-Serrano, S.M., Beguería, S., López-Moreno, J.I., 2010. A Multiscalar Drought Index Sensitive to Global Warming: The Standardized Precipitation Evapotranspiration Index. J. Clim. 23, 1696–1718. https://doi.org/10.1175/2009JCLI2909.1.

Webb, E.E., Alexander, H.D., Paulson, A.K., Loranty, M.M., DeMarco, J., Talucci, A.C., Spektor, V., Zimov, N., Lichstein, J.W., 2024. Fire-Induced Carbon Loss and Tree Mortality in Siberian Larch Forests. Geophys. Res. Lett. 51 (1). https://doi.org/10.1029/2023GL105216 e2023GL105216.

White, J.C., Hermosilla, T., Wulder, M.A., Coops, N.C., 2022. Mapping, validating, and interpreting spatio-temporal trends in post-disturbance forest recovery. Remote Sens. Environ. 271, 112904. https://doi.org/10.1016/j.rse.2022.112904.

Wilson, N., Bradstock, R., Bedward, M., 2021. Comparing forest carbon stock losses between logging and wildfire in forests with contrasting responses to fire. For. Ecol. Manag. 481, 118701. https://doi.org/10.1016/j.foreco.2020.118701.

Wirth, C., Lichstein, J.W., 2009. In: Wirth, C., Gleixner, G., Heimann, M. (Eds.), The Imprint of Species Turnover on Old-Growth Forest Carbon Balances - Insights From a Trait-Based Model of Forest Dynamics, in: Old-Growth Forests, 207. Springer Berlin Heidelberg, Berlin, Heidelberg, pp. 81–113. https://doi.org/10.1007/978-3-540-92706-8_5.

Wittenberg, L., Malkinson, D., Beeri, O., Halutzy, A., Tesler, N., 2007. Spatial and temporal patterns of vegetation recovery following sequences of forest fires in a Mediterranean landscape, Mt. Carmel Israel, CATENA 71, 76–83. https://doi.org/10.1016/j.catena.2006.10.007.

Wooten, J.T., Stevens-Rumann, C.S., Schapira, Z.H., Rocca, M.E., 2022. Microenvironment characteristics and early regeneration after the 2018 Spring Creek Wildfire and post-fire logging in Colorado, USA. Fire Ecol. 18 (1), 10. https://doi.org/10.1186/s42408-022-00133-8.

Wright, M.N., Ziegler, A., 2017. ranger: A fast implementation of random forests for high dimensional data in C++ and R. Int. J. Stat. Softw. 77, 1–17. https://doi.org/10.18637/jss.v077/i01.

Xu, R., Ye, T., Yue, X., Yang, Z., Yu, W., Zhang, Y., Bell, M.L., Morawska, L., Yu, P., Zhang, Y., Wu, Y., Liu, Y., Johnston, F., Lei, Y., Abramson, M.J., Guo, Y., Li, S., 2023. Global population exposure to landscape fire air pollution from 2000 to 2019. Nature 621 (7979), 521–529. https://doi.org/10.1038/s41586-023-06398-6.

Yilmaz, E., Ozdemir, E., Makineci, E., 2021. Bark thickness models for oak forests being converted from coppice to high forests in Northwestern Turkey. Environ. Monit. Assess. 193, 728. https://doi.org/10.1007/s10661-021-09524-x.

Yue, C., Ciais, P., Luyssaert, S., Cadule, P., Harden, J., Randerson, J., Bellassen, V., Wang, T., Piao, S.L., Poulter, B., Viovy, N., 2013. Simulating boreal forest carbon dynamics after stand-replacing fire disturbance: Insights from a global process-based vegetation model. Biogeosciences 10 (12), 8233–8252. https://doi.org/10.5194/bg-10-8233-2013.

Zribi, L., Mouillot, F., Guibal, F., Rejeb, S., Rejeb, M., Gharbi, F., 2016. Deep Soil Conditions Make Mediterranean Cork Oak Stem Growth Vulnerable to Autumnal Rainfall Decline in Tunisia. Forests 7 (10), 245. https://doi.org/10.3390/f7100245.